Recoil corrections in highly charged ions

G. S. Adkins*
Department of Physics, Franklin and Marshall College, Lancaster, Pennsylvania 17604, USA

S. Morrison† and J. Sapirstein‡
Department of Physics, University of Notre Dame, Notre Dame, Indiana 46556, USA

(Received 12 July 2007; published 10 October 2007)

A recently introduced Bethe-Salpeter formalism is applied to the calculation of recoil corrections to the energy levels of all $n=1$, 2, and 3 states of hydrogenic ions. Finite basis set techniques are shown to allow the accurate evaluation of expressions that sum all orders of $Z\alpha$, which are rederived in the formalism using combinatoric techniques. A comparison of the all-order results with one-loop calculations and known terms of the perturbation expansion in $Z\alpha$ is made. Good agreement of the results of the present work with previous calculations is shown, and a discussion of issues that will have to be treated for the many-electron case, where highly accurate experiments have been carried out, is given.

DOI: 10.1103/PhysRevA.76.042508 PACS number(s): 31.30.Jv, 12.20.Ds

I. INTRODUCTION

In a recent paper [1] a variant of a three-dimensional Bethe-Salpeter formalism introduced by Lepage [2] designed to reduce to the Dirac equation in the limit of infinite nuclear mass was introduced. Such a formalism is necessary for calculation of recoil corrections in highly charged hydrogenic ions, as the usual power series expansion in $Z\alpha$ becomes increasingly unreliable as Z increases. While high Z necessarily goes along with very small mass ratios m/M, where m is the electron mass and M is the nuclear mass, recent experiments in highly charged lithiumlike [3], sodiumlike [4], and copperlike [5] ions have reached the tenth of an eV level, smaller than the effect of recoil, so a relativistic calculation of recoil is necessary. While similar precision has not been achieved for hydrogenic ions, the present calculation can still be applied to the many-electron case, as at high Z the wave function can be approximated as a product of hydrogenic orbitals. Further discussion of this point is given in the concluding section.

In Ref. [1] we were concerned with setting up the formalism, and carried out only one part of the calculation, the one-transverse photon exchange contribution to the ground state energy, for a range of Z's. We instead concentrated on the subset of graphs that contributed to the known recoil corrections to fine structure of order $m^2(Z\alpha)^4/M$. In the present paper we consider a more complete set of diagrams in a slightly modified formalism. We begin by calculating all two-photon exchange diagrams, which in Coulomb gauge requires the treatment of Coulomb-Coulomb, Coulomb-transverse, and transverse-transverse photon exchanges. These terms start in order $m^2(Z\alpha)^5/M$, the calculation of which was first carried out by Salpeter [6]. The calculations presented here include all higher-order corrections of order $m^2(Z\alpha)^n/M$, since the formalism is relativistic and the integrals are carried out numerically. As in the previous work, we neglect all terms with an additional factor of m/M, as these are entirely negligible for the heavy ions we are concerned with.

Three and higher photon exchange diagrams, in which one of the photons exchanged is transverse, also enter in order $m^2(Z\alpha)^5/M$. In addition, such diagrams in which all the photons are Coulomb start in order $m^2(Z\alpha)^6/M$. While the analysis of these infinite sets of diagrams, first carried out by Braun [7] and by Shabaev [8], is quite complicated, the end expression is fairly simple. When two transverse photons along with any number of Coulomb photons are exchanged, another infinite set of diagrams must be considered. In all three cases it is convenient to also include the one-loop result, in which case the complete result can be expressed in terms of the Dirac-Coulomb propagator, which satisfies the equation

$$\left[E\gamma_0 + i\vec{\gamma}\cdot\vec{\nabla} + \frac{Z\alpha}{r}\gamma_0 - m\right]S_F(E;\vec{x},\vec{y}) = \delta^3(\vec{x}-\vec{y}). \quad (1)$$

We evaluate the terms involving the Dirac-Coulomb propagator by using its spectral representation,

$$S_F(E;\vec{x},\vec{y}) = \sum_m \frac{\psi_m(\vec{x})\bar{\psi}_m(\vec{y})}{E-\mathcal{E}_m(1-i\epsilon)}, \quad (2)$$

together with finite basis set techniques [9,10], described in more detail below.

We consider all $n=1$, 2, and 3 states in this paper for a range of nuclear charges. As mentioned above, high precision experiments on highly charged lithiumlike [3] and sodiumlike [4] ions have reached precisions where these small recoil effects must be treated. The $n=4$ case, needed for interpretation of copperlike ions [5], along with recoil corrections associated with mass polarization will be treated elsewhere.

The plan of the paper is as follows. We briefly reprise the formalism introduced in Ref. [1] in the next section. The modification of that formalism mentioned above turns out to be necessary to properly treat the all-Coulomb problem, and

*gadkins@fandm.edu
†smorriso@nd.edu
‡jsapirst@nd.edu

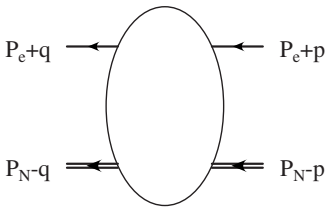

FIG. 1. Momentum assignments for electron-nucleus two-particle diagrams. The electron-line momentum is $P_e=(E,\vec{0})$ and the nucleus-line momentum is $P_N=(M,\vec{0})$. The initial and final relative momenta are p and q.

details of that modification will be given. In the next three sections we evaluate one-photon, two-photon, and three-photon exchange diagrams in turn. In the last case we show that certain expressions involving the one-potential part of the Dirac-Coulomb propagator arise. This one-potential part in fact turns into the complete Dirac-Coulomb propagator when four and higher photon exchange diagrams are considered. The rather complicated combinatoric proof of this is given in the Appendix. In the next section we describe the techniques we use to numerically evaluate the terms involving the Dirac-Coulomb propagator, and tabulate the total recoil contribution for the nine states with principal quantum numbers $n=1-3$ for the isoelectronic sequence. The breakdown of the total result is illustrated for the case $Z=92$. In the Conclusion we compare our results, where possible, with previous calculations by Artemyev *et al.* [11,12], and discuss issues that will arise for the many-electron case.

II. FORMALISM

There are many ways to set up three-dimensional forms of the Bethe-Salpeter equation, with the main point being the freedom to replace the fully relativistic propagator of two particles, $\bar{S}(k)$, with a simpler form, $\tilde{S}(k)\equiv NS(\vec{k})\delta(k_0-A)$. $\bar{S}(k)$ itself has some freedom associated with it, as the momentum entering and leaving a diagram involving $\bar{S}(k)$ in the center of mass system can be chosen in different ways. We choose the momentum routing indicated in Fig. 1. Here $P_e=(E,\vec{0})$ and $P_N=(M,\vec{0})$ build in the main part of the energies of the electron and nuclear lines, respectively, and the total energy of the system is $M+E$. In the following, for convenience, when we refer to the total energy the contribution M will be understood to be included, even though it is not explicitly written. The momentum routing we have chosen leads to an interior electron-nucleus propagator

$$\bar{S}(k)=\frac{i}{\gamma(P_e+k)-m+i\epsilon}\frac{i}{(P_N-k)^2-M^2+i\epsilon}. \tag{3}$$

For a heavy nucleus the nuclear propagator is peaked at small k_0. In our original formalism [1], we chose $\tilde{S}(k)$ to make k_0 precisely 0, in addition choosing $p_0=q_0=0$. However, this choice, which keeps the nucleus off mass shell, turns out to have poor behavior once loops with Coulomb photons are considered. Here we will instead choose a routing that puts the nucleus on mass shell to order $1/M^2$, which eliminates this poor behavior. We also used $P_e=(\frac{\mu}{m}E,\vec{0})$, $P_N=(M+m-\mu,\vec{0})$ in order to build the reduced mass μ into the lowest order problem: our present choice makes the lowest order problem completely nonrecoil, and all recoil effects will be treated perturbatively.

In order to keep intermediate nuclear propagators on mass shell, we choose a reference propagator

$$\tilde{S}(k)=\frac{\pi\delta\left(k_0+\frac{\vec{k}^2}{2M}\right)}{M}\frac{i}{\left(E-\frac{\vec{k}^2}{2M}\right)\gamma_0-\vec{\gamma}\cdot\vec{k}-m+i\epsilon}$$
$$\equiv\frac{i\pi\delta\left(k_0+\frac{\vec{k}^2}{2M}\right)}{M}S(\vec{k}). \tag{4}$$

At this point we also choose $p=(-\vec{p}^2/2M,\vec{p})$ and $q=(-\vec{q}^2/2M,\vec{q})$, which puts the nuclear lines on shell to order $1/M^2$. We use this reference propagator to define a modified kernel for the truncated form of the Bethe-Salpeter equation,

$$\bar{G}_T(E;q,p)=i\bar{K}(E;q,p)+\int\frac{d^4k}{(2\pi)^4}\bar{K}(E;q,k)\bar{S}(k)\bar{G}_T(E;k,p), \tag{5}$$

through

$$\bar{G}_T(E;q,p)=i\tilde{K}(E;q,p)+\int\frac{d^4k}{(2\pi)^4}\tilde{K}(E;q,k)\tilde{S}(k)\bar{G}_T(E;k,p). \tag{6}$$

The modified kernel can be expanded as

$$\tilde{K}(E;q,p)=\bar{K}(E;q,p)+\int\frac{d^4k}{(2\pi)^4}\bar{K}(E;q,k)[\bar{S}(k)-\tilde{S}(k)]$$
$$\times\bar{K}(E;k,p)+\int\frac{d^4k}{(2\pi)^4}\int\frac{d^4l}{(2\pi)^4}\bar{K}(E;q,k)$$
$$\times[\bar{S}(k)-\tilde{S}(k)]\bar{K}(E;k,l)[\bar{S}(l)-\tilde{S}(l)]\bar{K}(E;l,p)$$
$$+\cdots. \tag{7}$$

Because of the delta function in $\tilde{S}(k)$ and the routing of momentum we have chosen, Eq. (6) can be written in a three-dimensional form,

$$G_T(E;\vec{q},\vec{p})=iK(E;\vec{q},\vec{p})$$
$$+\frac{1}{2M}\int\frac{d^3k}{(2\pi)^3}iK(E;\vec{q},\vec{k})S(\vec{k})G_T(E;\vec{k},\vec{p}), \tag{8}$$

where

$$G_T(E;\vec{q},\vec{p})=\bar{G}_T\left(E;-\frac{\vec{q}^2}{2M},\vec{q},-\frac{\vec{p}^2}{2M},\vec{p}\right) \tag{9}$$

and

$$K(E;\vec{q},\vec{p}) = \tilde{K}\left(E;-\frac{\vec{q}^2}{2M},\vec{q},-\frac{\vec{p}^2}{2M},\vec{p}\right). \tag{10}$$

We next create an untruncated Green's function

$$G(E;\vec{q},\vec{p}) = \frac{1}{2M}S(\vec{q})(2\pi)^3\delta^3(\vec{q}-\vec{p}) + \frac{1}{4M^2}S(\vec{q})G_T(E;\vec{q},\vec{p})S(\vec{p}). \tag{11}$$

While not equal to the Bethe-Salpeter untruncated Green's function, its poles are at the same position. It satisfies the equation

$$\left[\left(E-\frac{\vec{q}^2}{2M}\right)\gamma_0 - \vec{\gamma}\cdot\vec{q} - m\right]G(E;\vec{q},\vec{p}) = \frac{1}{2M}(2\pi)^3\delta^3(\vec{q}-\vec{p}) + \frac{1}{2M}\int\frac{d^3k}{(2\pi)^3}iK(E;\vec{q},\vec{k})G(E;\vec{k},\vec{p}). \tag{12}$$

If we move the $\frac{\vec{q}^2}{2M}\gamma_0$ term to the right hand side of the equation we can identify it as an additional kernel we call iK_A, with

$$iK_A(E;\vec{q},\vec{k}) = (2\pi)^3\delta^3(\vec{q}-\vec{k})\vec{q}^2\gamma_0, \tag{13}$$

after which we can drop that term in Eq. (12). This effect is also derived in the Appendix, Eq. (A21).

We now replace $K(E;\vec{q},\vec{k})$ with an approximation to one-Coulomb photon exchange,

$$K_{1C}(\vec{q},\vec{k}) = \frac{4\pi i Z\alpha}{|\vec{q}-\vec{k}|^2}2M\gamma_0. \tag{14}$$

The approximation made is to use $2M$ in the numerator: the complete one-Coulomb kernel has other terms which contribute in a higher order of m/M than we are considering here. Again noting that the $\vec{q}^2/2M$ term in Eq. (12) is now being treated as a kernel, we find that the equation in this approximation becomes

$$(E\gamma_0 - \vec{\gamma}\cdot\vec{q} - m)G_0(E;\vec{q},\vec{p}) = \frac{1}{2M}(2\pi)^3\delta^3(\vec{q}-\vec{p}) - \int\frac{d^3k}{(2\pi)^3}\frac{4\pi Z\alpha}{|\vec{q}-\vec{k}|^2}\gamma_0 G_0(E;\vec{k},\vec{p}), \tag{15}$$

which we recognize as a scaled version of the momentum space form of Eq. (1), having poles at the Dirac energies $\mathcal{E}_0$. Therefore our lowest order energy for a state with principal quantum number n, angular momentum quantum number κ, and $j=|\kappa|-1/2$ is

$$\mathcal{E}_0 = mf(n,j), \tag{16}$$

where

$$f(n,j) = \left[1+\left(\frac{Z\alpha}{n-(j+1/2)+\sqrt{(j+1/2)^2-(Z\alpha)^2}}\right)^2\right]^{-1/2}. \tag{17}$$

The residue of the Green's function is a product of Dirac wave functions scaled with a factor $\frac{1}{2M}$. It is convenient to work with the usual Dirac wave functions, and simply move the factor into the formulas for energy shifts: in particular, first-order perturbation theory can be written as

$$\mathcal{E}_1 - \mathcal{E}_0 \equiv \Delta E_1 = \frac{1}{2M}\int\frac{d^3kd^3l}{(2\pi)^6}\bar{\psi}(\vec{k})[i\bar{K}(\mathcal{E}_0;\vec{k},\vec{l}) - iK_{1C}(\vec{k},\vec{l})]\psi(\vec{l}). \tag{18}$$

This is to be combined with the shift from the kernel K_A,

$$\Delta E_A = \int\frac{d^3k}{(2\pi)^3}\psi^\dagger(\vec{k})\frac{\vec{k}^2}{2M}\psi(\vec{k}). \tag{19}$$

In our previous work [1] terms of order $m^2(Z\alpha)^4/M$ arose from one transverse photon exchange $(1T)$ diagrams and one-loop diagrams involving Coulomb photons. In the present formalism the one-loop diagrams do not contribute to this order, as the subtraction from $\bar{S}-\tilde{S}$ in Eq. (7) is finer, and all such terms come from ΔE_A and ΔE_{1T}. All remaining effects are of order $m^2(Z\alpha)^5/M$ and higher. We write the total energy as

$$\begin{aligned}\mathcal{E} &= mf(n,j) + \frac{m^2(Z\alpha)^2}{2Mn^2} + \frac{m^2(Z\alpha)^4}{M}\left(-\frac{1}{8n^4} + \left[\frac{1}{2n^3(j+1/2)} - \frac{3}{8n^4}\right]\right) + \frac{m^2(Z\alpha)^5}{M}R(n,\kappa,Z\alpha)\\ &= mf(n,j) + \frac{m^2(Z\alpha)^2}{2Mn^2} + \frac{m^2(Z\alpha)^4}{M}\left(-\frac{1}{2n^4} + \frac{1}{2n^3(j+1/2)}\right) + \frac{m^2(Z\alpha)^5}{M}R(n,\kappa,Z\alpha),\end{aligned} \tag{20}$$

where we have put the fine structure part of the $m^2(Z\alpha)^4/M$ term in square brackets in the first line to emphasize that it could be accounted for by using the reduced mass rather than the electron mass in the term $mf(n,j)$. We note that one frequently encounters this parametrization, in which case the third term has only the $-\frac{1}{8n^4}$ factor. This choice requires us to subtract out contributions of order $m^2(Z\alpha)^2/M$ and $m^2(Z\alpha)^4/M$ from ΔE_A, and contributions of order $m^2(Z\alpha)^4/M$ from ΔE_{1T}, after which we absorb the remainder into $R(n,\kappa,Z\alpha)$. We illustrate this procedure with ΔE_A. This energy shift, evaluated in the "valence" state v, is

$$\begin{aligned}\Delta E_A &= \frac{1}{2M}\int\frac{d^3k}{(2\pi)^3}\psi_v^\dagger(\vec{k})\vec{k}^2\psi_v(\vec{k})\\ &= \frac{1}{2M}\int\frac{d^3k}{(2\pi)^3}\psi_v^\dagger(\vec{k})\vec{\alpha}\cdot\vec{k}\vec{\alpha}\cdot\vec{k}\psi_v(\vec{k})\\ &= \frac{1}{2M}\left\langle v\left|\left(H-\beta m+\frac{Z\alpha}{r}\right)\left(H-\beta m+\frac{Z\alpha}{r}\right)\right|v\right\rangle\end{aligned}$$

TABLE I. Lower-order contributions to ΔE_A and ΔE_{1T} by state.

State	$\frac{m^2(Z\alpha)^2}{M}\Delta E_A$ coefficient	$\frac{m^2(Z\alpha)^4}{M}\Delta E_A$ coefficient	$\frac{m^2(Z\alpha)^4}{M}\Delta E_{1T}$ coefficient
$1s$	$\frac{1}{2}$	1	-1
$2s$	$\frac{1}{8}$	$\frac{7}{32}$	$-\frac{3}{16}$
$2p_{1/2}$	$\frac{1}{8}$	$\frac{13}{96}$	$-\frac{5}{48}$
$2p_{3/2}$	$\frac{1}{8}$	$\frac{1}{24}$	$-\frac{1}{24}$
$3s$	$\frac{1}{18}$	$\frac{2}{27}$	$-\frac{5}{81}$
$3p_{1/2}$	$\frac{1}{18}$	$\frac{4}{81}$	$-\frac{1}{27}$
$3p_{3/2}$	$\frac{1}{18}$	$\frac{7}{324}$	$-\frac{1}{54}$
$3d_{3/2}$	$\frac{1}{18}$	$\frac{1}{60}$	$-\frac{11}{810}$
$3d_{5/2}$	$\frac{1}{18}$	$\frac{1}{135}$	$-\frac{1}{135}$

$$= \frac{1}{2M}\left(\mathcal{E}_{0v}^2 - 2\mathcal{E}_{0v}m\langle v|\beta|v\rangle + 2\mathcal{E}_{0v}Z\alpha\left\langle v\left|\frac{1}{r}\right|v\right\rangle + m^2 - 2mZ\alpha\left\langle v\left|\frac{\beta}{r}\right|v\right\rangle + (Z\alpha)^2\left\langle v\left|\frac{1}{r^2}\right|v\right\rangle\right). \tag{21}$$

For the ground state, where $f(1,\frac{1}{2})=\sqrt{1-(Z\alpha)^2}\equiv\gamma$, this gives

$$\Delta E_A(1s) = \frac{(mZ\alpha)^2}{2M}\left[1+\frac{2(Z\alpha)^2}{\gamma(2\gamma-1)}\right] = \frac{m^2(Z\alpha)^2}{2M} + \frac{m^2(Z\alpha)^4}{M} + \frac{m^2(Z\alpha)^5}{M}\frac{(1-\gamma)(1+2\gamma)}{\gamma(2\gamma-1)Z\alpha}, \tag{22}$$

and we include the last term in $R(1,-1,Z\alpha)$. We note in advance that ΔE_{1T} for the ground state has a contribution of $-\frac{m^2(Z\alpha)^4}{M}$, which cancels the term of this order in ΔE_A, in accordance with Eq. (20). In fact, the cancellation works to all orders for the ground state, as by using virial relations it is possible to show [8] for the point Dirac case that

$$\Delta E_A + \Delta E_{1T} = \frac{m^2-\mathcal{E}_0^2}{2M}, \tag{23}$$

and this is exactly $\frac{m^2(Z\alpha)^2}{2M}$ for the ground state. However, we arrange the calculation in a slightly different fashion that allows extension to the non-Coulomb problem. Once one has the Dirac wave function in momentum space, the evaluation of the expectation value of $\vec{k}^2/(2M)$ is easily carried out numerically. We subtract from this the known terms of order $m^2(Z\alpha)^2/M$ and $m^2(Z\alpha)^4/M$, tabulated in the second and third columns of Table I, and present the contribution of the remainder to $R(n,\kappa,Z\alpha)$ for $Z=92$ in the second column of Table II. We now turn to a discussion of one-photon, two-photon, and three-photon kernels, with the latter being generalized to all orders in the Appendix.

III. ONE-PHOTON EXCHANGE

The next simplest perturbation is that of one-transverse photon exchange, which, as mentioned above, contributes in order $m^2(Z\alpha)^4/M$. Because we are now interested in more than the ground state, a new angular momentum issue must be addressed. If we represent a general wave function in momentum space by

$$\psi(\vec{p}) = (mZ\alpha)^{-3/2}\begin{pmatrix} g(p)\chi_{\kappa\mu}(\hat{p}) \\ f(p)\chi_{-\kappa\mu}(\hat{p}) \end{pmatrix}, \tag{24}$$

TABLE II. Breakdown of contributions to $R(n,\kappa,Z\alpha)$ for $Z=92$ for all $n=1$, 2, and 3 states of hydrogenic ions.

Z	ΔE_A	ΔE_{1T}	ΔE_{CC}	ΔE_{CT}	ΔE_{TT}	$\Delta E'_{CC}$	$\Delta E'_{CT}$	$\Delta E'_{TT}$	Sum
$1s$	2.6778	−2.6778	−1.7341	2.9652	−0.3179	1.1446	−0.8922	0.3518	1.5174
$2s$	0.6418	−0.6268	−0.3068	0.5125	−0.0356	0.2027	−0.1210	0.0693	0.3361
$2p_{1/2}$	0.2492	−0.2343	−0.0438	0.0052	0.0116	0.0258	0.0198	0.0468	0.0803
$2p_{3/2}$	0.0093	−0.0093	−0.0004	−0.0102	−0.0038	0.0001	0.0207	0.0015	0.0079
$3s$	0.1967	−0.1911	−0.0907	0.1521	−0.0096	0.0598	−0.0344	0.0209	0.1037
$3p_{1/2}$	0.0841	−0.0784	−0.0150	0.0049	0.0043	0.0085	0.0048	0.0156	0.0288
$3p_{3/2}$	0.0056	−0.0053	−0.0001	−0.0028	−0.0009	0.0000	0.0066	0.0010	0.0041
$3d_{3/2}$	0.0037	−0.0034	0.0000	−0.0011	−0.0002	0.0000	0.0010	0.0007	0.0007
$3d_{5/2}$	0.0007	−0.0007	0.0000	−0.0006	−0.0003	0.0000	0.0011	0.0002	0.0004

we encounter structures of the form $\chi^{\dagger}_{\kappa\mu}(\hat{l})\chi_{\kappa\mu}(\hat{k})$. When $\kappa=\pm 1$ these are easily analyzed using $\vec{\sigma}\cdot\hat{k}\chi_{\kappa\mu}(\hat{k})=-\chi_{-\kappa\mu}(\hat{k})$, but for other values of κ we use an averaging procedure over the magnetic quantum numbers. It is straightforward to show that $\chi^{\dagger}_{\kappa\mu}(\hat{l})\chi_{\kappa\mu}(\hat{k})$ can be replaced with $P_{\ell}(z_3)/4\pi$, with ℓ being κ for positive κ and $-\kappa-1$ for negative κ, and $z_3=\hat{k}\cdot\hat{l}$. The energy shift for one transverse photon exchange is

$$\Delta E_{1T}=\frac{m^2(Z\alpha)^3}{32\pi^5 M}\int d^3k\int d^3l\left(\frac{T_A[kg(l)f(k)+lf(l)g(k)]+T_B[lg(l)f(k)+kf(l)g(k)]}{|\vec{l}-\vec{k}|^2}+(\vec{k}^2-\vec{l}^2)\right.$$
$$\left.\times\frac{T_A[-kg(l)f(k)+lf(l)g(k)]+T_B[lg(l)f(k)-kf(l)g(k)]}{|\vec{l}-\vec{k}|^4}\right), \tag{25}$$

where T_A is the appropriate Legendre polynomial for κ and T_B for $-\kappa$. This expression was exact in our previous formalism, which forced the time component of the photon propagator to vanish. However, while in the present formalism it is nonzero, its magnitude is order $1/M$, and because one transverse photon exchange starts in order $1/M$, we can still use this equation. This becomes a three-dimensional integral over z_3 and the magnitudes of $\vec{k}$ and $\vec{l}$, which can be evaluated using the adaptive multidimensional integration program VEGAS [13]. For the point Coulomb case the integral can also be done analytically [8], and the results agree within numerical errors. The $m^2(Z\alpha)^4/M$ part of the $1T$ perturbation, tabulated in the fourth column of Table I, is removed, and the contribution of the remaining terms to the function $R(n,j,Z\alpha)$ are tabulated in the third column of Table II. We note the exact cancellation between ΔE_A and ΔE_{1T} for the $1s$, $2p_{3/2}$, and $3d_{5/2}$ states.

IV. TWO-PHOTON EXCHANGE KERNELS

We next consider diagrams with two Coulomb photons, shown in Figs. 2(a)–2(c), referred to in the following as the Coulomb ladder, crossed Coulomb ladder, and seagull graphs. Our convention is that Coulomb photons are represented by dashed lines and transverse photons by wiggly lines. We illustrate the technique we use to evaluate them with the crossed Coulomb graph. As discussed in our previous paper, when the fourth component of the internal loop momentum is carried out with Cauchy's theorem, the only pole that needs to be considered is that from the electron propagator, which gives

$$\Delta E_{CCX}=\frac{(Z\alpha)^2}{128\pi^7 M}\int\frac{d^3kd^3qd^3l}{|\vec{q}-\vec{k}|^2|\vec{q}-\vec{l}|^2}\left(2M+q_0^a+\frac{\vec{k}^2+2\vec{l}^2}{2M}\right)\left(2M+q_0^a+\frac{2\vec{k}^2+\vec{l}^2}{2M}\right)$$
$$\times\frac{\psi^{\dagger}(\vec{l})[(\mathcal{E}_0+q_0^a)\gamma_0-\vec{\gamma}\cdot\vec{q}+m]\gamma_0\psi(\vec{k})}{\sqrt{\vec{q}^2+m^2}\left[\left(q_0^a+\frac{\vec{k}^2+\vec{l}^2}{2M}+M\right)^2-M^2-|\vec{q}-\vec{k}-\vec{l}|^2\right]}, \tag{26}$$

where $q_0^a=-\mathcal{E}_0-\sqrt{\vec{q}^2+m^2}$. This term is of order m^2/M, so the $1/M$ terms in the numerator can be dropped, giving

$$\Delta E_{CCX}=\frac{(Z\alpha)^2}{128\pi^7 M}\int\frac{d^3kd^3qd^3l}{|\vec{q}-\vec{k}|^2|\vec{q}-\vec{l}|^2}\frac{(2M+q_0^a)(2M+q_0^a)\psi^{\dagger}(\vec{l})[(\mathcal{E}_0+q_0^a)\gamma_0-\vec{\gamma}\cdot\vec{q}+m]\gamma_0\psi(\vec{k})}{\sqrt{\vec{q}^2+m^2}\left[\left(q_0^a+\frac{\vec{k}^2+\vec{l}^2}{2M}+M\right)^2-M^2-|\vec{q}-\vec{k}-\vec{l}|^2\right]}. \tag{27}$$

This nominally nine-dimensional integral becomes a six-dimensional integral after orienting $\vec{q}$ along the z axis and choosing $\vec{k}$ to lie in the $x-z$ plane. We set $k_z=k\cos\theta_1$, $k_x=k\sin\theta_1$, $l_z=l\cos\theta_2$, $l_x=l\sin\theta_2\cos\phi$, and $l_y=l\sin\theta_2\sin\phi$. At this point we must deal with a new kind of angular momentum structure. While $\chi^{\dagger}_{\kappa}(\hat{l})\chi_{\kappa}(\hat{k})$ can still be replaced by $P_{\ell}(\hat{l}\cdot\hat{k})/4\pi$, as with the one-transverse photon calculation, we now encounter terms in which $\vec{\sigma}\cdot\vec{q}$ is sandwiched between spherical spinors of equal and opposite κ values. To evaluate these terms we average over magnetic

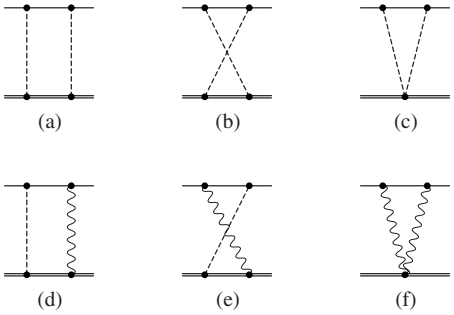

FIG. 2. The one-loop graphs. These are the (a) Coulomb ladder, (b) Coulomb crossed ladder, (c) Coulomb seagull, (d) Coulomb-transverse ladder, (e) Coulomb-transverse crossed ladder, and (f) transverse seagull graphs.

quantum numbers (suppressed in the following), to find

$$\chi_{-3}^{\dagger}(\hat{l})\vec{\sigma}\cdot\vec{q}\chi_3(\hat{k}) = \frac{q(z_1+2z_2z_3-5z_1z_3^2)}{8\pi},$$

$$\chi_{-2}^{\dagger}(\hat{l})\vec{\sigma}\cdot\vec{q}\chi_2(\hat{k}) = \frac{q(z_2-3z_1z_3)}{8\pi},$$

$$\chi_{-1}^{\dagger}(\hat{l})\vec{\sigma}\cdot\vec{q}\chi_1(\hat{k}) = -\frac{qz_1}{4\pi},$$

$$\chi_{1}^{\dagger}(\hat{l})\vec{\sigma}\cdot\vec{q}\chi_{-1}(\hat{k}) = -\frac{qz_2}{4\pi},$$

$$\chi_{2}^{\dagger}(\hat{l})\vec{\sigma}\cdot\vec{q}\chi_{-2}(\hat{k}) = \frac{q(z_1-3z_2z_3)}{8\pi},$$

$$\chi_{3}^{\dagger}(\hat{l})\vec{\sigma}\cdot\vec{q}\chi_{-3}(\hat{k}) = \frac{q(z_2+2z_1z_3-5z_2z_3^2)}{8\pi}, \tag{28}$$

where $z_1=\cos\theta_1$, $z_2=\cos\theta_2$, and $z_3=z_1z_2+\sin\theta_1\sin\theta_2\cos\phi$. The Coulomb ladder schematically comes from the term $K_C(S-S_0)K_C$, where S_0 cancels with a term in the S term involving taking the nuclear pole. In our previous formalism [1] this term contributed to order $m^2(Z\alpha)^4/M$, but in the present formalism the cancellation is more complete, leading to negligible terms of higher order in m/M. However, the electron pole contributes to R, and we combine it with the electron poles from the other two graphs, and present the sum in the fourth column of Table II.

The next diagrams we treat are one-Coulomb one-transverse diagrams in either a ladder or crossed ladder configuration, shown in Figs. 2(d) and 2(e), respectively. The transverse photon propagator in momentum space is proportional to the frequently encountered object

$$D_{ij}(k) = \left(\delta_{ij}-\frac{k_ik_j}{\vec{k}^2}\right)\frac{1}{k_0^2-\vec{k}^2+i\epsilon}. \tag{29}$$

The ladder diagram by itself is of the order of the $1T$ diagram, but the formalism subtracts out that contribution, leaving a correction of order $m^2(Z\alpha)^5/M$; the crossed diagram is not subtracted, and is of the same order. Combining the two graphs leads to greater numerical stability than when they are evaluated separately. The results are given in the fifth column of Table II.

A simplification present in our formalism is the fact that two-transverse photon diagrams of the ladder and crossed ladder category contribute in order m^3/M^2, and can therefore be ignored. Were the nucleus treated as a Dirac particle these diagrams would play a central role, but here the seagull diagram, shown in Fig. 2(f), is all that need be considered, and its contribution is

$$\Delta E_{TT} = \frac{(4\pi Z\alpha)^2 i}{M}\int\frac{d^3kd^3qd^3l}{(2\pi)^9} \times\int\frac{dq_0}{2\pi}D_{ik}(q_1)D_{jk}(q_2)\bar{\psi}(\vec{l})\gamma_iS_0(\mathcal{E}_0+q_0,\vec{q})\gamma_j\psi(\vec{k}), \tag{30}$$

where $\vec{q}_1=\vec{q}-\vec{l}$, $\vec{q}_2=\vec{q}-\vec{k}$, and $q_{10}=q_{20}=q_0$, where the approximation of working to first order in recoil has been used in the last equation. Carrying out the q_0 integral with Cauchy's theorem results in three poles, and the remaining six-dimensional integral is carried out with VEGAS. The results are tabulated in the sixth column of Table II. At this point all $m^2(Z\alpha)^5/M\ \ln Z\alpha$ terms, specifically $-\frac{2}{3\pi\pi^3}\delta_{l0}\ln Z\alpha$ in terms of $R(n,j,Z\alpha)$, are accounted for. However, the constant is not complete, as it has contributions from multiloop graphs, to which we now turn.

V. THREE-PHOTON EXCHANGE KERNELS

Our strategy in this section is to analyze three-photon exchange kernels in a manner that generalizes the approach in our previous paper [1], where we treated one-transverse–two-Coulomb photon exchange diagrams, which contribute a constant term to order $m^2(Z\alpha)^5/M$ that can be identified with part of the Bethe logarithm. We showed that the one-potential part of the Dirac-Coulomb propagator,

$$S_{1C}(E;\vec{k},\vec{l}) = S_0(E;\vec{k})\frac{-4\pi Z\alpha}{|\vec{k}-\vec{l}|^2}\gamma_0S_0(E;\vec{l}), \tag{31}$$

arose when the transverse photon pole was taken, and then found that the standard form first found by Salpeter [6] came from replacing S_{1C} with the full Dirac-Coulomb propagator S_F. We repeat and generalize this analysis in this section in order to motivate the all-orders expressions associated with firstly, all-Coulomb terms, then two-transverse photon exchange terms with an arbitrary number of Coulomb exchanges, and finally, one transverse photon with any number of Coulomb photon terms. We give a more rigorous derivation, using a somewhat different formalism, in the Appendix. We note that a similar analysis has been given by Doncheski, Grotch, and Erickson in Ref. [14].

A. Coulomb photon exchange terms

The most complicated all-orders work encountered here has to do with summing the infinite set of Coulomb exchanges. While the $(Z\alpha)^2\frac{m^2}{M}$, $(Z\alpha)^4\frac{m^2}{M}$, and $(Z\alpha)^5\frac{m^2}{M}$ terms are accounted for by the one-loop calculation, terms of higher order, which of course are not necessarily small at high Z, come from all two- and higher-loop diagrams. In this section we treat three-Coulomb photon exchange, and show that it can be written in terms of a rather simple formula involving S_{1C}.

We first consider the six three-photon diagrams when no seagull is present, shown in Fig. 3. We follow the notation of Ref. [15], where diagram 3(a) was called X, diagrams 3(b) and 3(c) were called Z, and diagrams 3(d) and 3(e) were called Y. We use L for diagram 3(f) instead of the previously used 0 for notational clarity. We route the momentum so that the electron line always has the same form. The contribution to the energy of the X diagram is

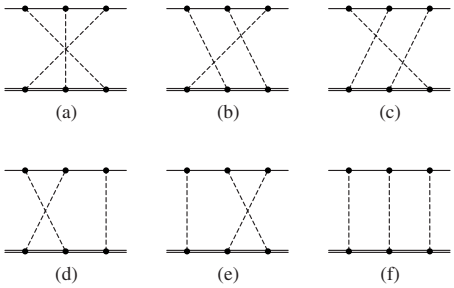

FIG. 3. Nonseagull two-loop graphs.

$$\Delta E_X = \frac{(4\pi Z\alpha)^3}{2M(2\pi)^{12}}\int \frac{d^3k d^3q d^3r d^3l}{|\vec{k}-\vec{q}|^2|\vec{q}-\vec{r}|^2|\vec{r}-\vec{l}|^2}\frac{dq_0}{2\pi}\frac{dr_0}{2\pi}\bar{\psi}(\vec{l})\gamma_0 S_0(\mathcal{E}_0+r_0;\vec{r})\gamma_0 S_0(\mathcal{E}_0+q_0;\vec{q})\gamma_0\psi(\vec{k})$$
$$\times\frac{\left(2M+\frac{2\vec{l}^2+\vec{k}^2}{2M}+q_0\right)\left(2M+\frac{\vec{k}^2+\vec{l}^2}{M}+r_0+q_0\right)\left(2M+\frac{2\vec{k}^2+\vec{l}^2}{2M}+r_0\right)}{\left[\left(M+\frac{\vec{l}^2+\vec{k}^2}{2M}+q_0\right)^2-M^2-|\vec{q}-\vec{l}-\vec{k}|^2+i\epsilon\right]\left[\left(M+\frac{\vec{k}^2+\vec{l}^2}{2M}+r_0\right)^2-M^2-|\vec{r}-\vec{l}-\vec{k}|^2+i\epsilon\right]}. \tag{32}$$

This expression is exact. Because we are dropping terms of order m^3/M^2, we can make the approximation

$$\Delta E_X = \frac{(4\pi Z\alpha)^3}{(2\pi)^{12}}\int \frac{d^3k d^3q d^3r d^3l}{|\vec{k}-\vec{q}|^2|\vec{q}-\vec{r}|^2|\vec{r}-\vec{l}|^2}\frac{dq_0}{2\pi}\frac{dr_0}{2\pi}\bar{\psi}(\vec{l})\gamma_0 S_0(\mathcal{E}_0+r_0;\vec{r})\gamma_0 S_0(\mathcal{E}_0+q_0;\vec{q})\gamma_0\psi(\vec{k})$$
$$\times\frac{\left(1+\frac{q_0}{2M}\right)\left(1+\frac{r_0+q_0}{2M}\right)\left(1+\frac{r_0}{2M}\right)}{\left[\left(q_0+\frac{\vec{l}^2+\vec{k}^2+q_0^2}{2M}\right)-\frac{|\vec{q}-\vec{l}-\vec{k}|^2}{2M}+i\epsilon\right]\left[\left(r_0+\frac{\vec{k}^2+\vec{l}^2+r_0^2}{2M}\right)-\frac{|\vec{r}-\vec{l}-\vec{k}|^2}{2M}+i\epsilon\right]}$$
$$\doteq\frac{\left(1+\frac{q_0}{2M}\right)\left(1+\frac{r_0+q_0}{2M}\right)\left(1+\frac{r_0}{2M}\right)}{\left[\left(q_0+\frac{\vec{l}^2+\vec{k}^2+q_0^2}{2M}\right)-\frac{|\vec{q}-\vec{l}-\vec{k}|^2}{2M}+i\epsilon\right]\left[\left(r_0+\frac{\vec{k}^2+\vec{l}^2+r_0^2}{2M}\right)-\frac{|\vec{r}-\vec{l}-\vec{k}|^2}{2M}+i\epsilon\right]}, \tag{33}$$

where we use the $\doteq$ symbol to indicate that the first line of the above equation, which is the same for all diagrams, is understood. If we now use

$$\frac{1}{q_0+\frac{A}{M}+i\epsilon}=\frac{1}{q_0+i\epsilon}-\frac{A}{M}\frac{1}{(q_0+i\epsilon)^2}, \tag{34}$$

valid because we are working only to order m^2/M, we have

$$\Delta E_X \doteq \frac{1}{(q_0+i\epsilon)(r_0+i\epsilon)}\left(1+\frac{q_0+r_0}{M}\right)-\frac{1}{2M}\frac{1}{(q_0+i\epsilon)^2}\frac{1}{r_0+i\epsilon}(\vec{l}^2+\vec{k}^2+q_0^2-|\vec{q}-\vec{l}-\vec{k}|^2)-\frac{1}{2M}\frac{1}{q_0+i\epsilon}\frac{1}{(r_0+i\epsilon)^2}(\vec{l}^2+\vec{k}^2+r_0^2$$
$$-|\vec{r}-\vec{l}-\vec{k}|^2). \tag{35}$$

We now turn to the Z graphs, which are mirror images of one another. We find for Figs. 3(b) and 3(c) the results

$$\Delta E_{Z1} \doteq \frac{\left(1+\frac{q_0}{2M}\right)\left(1+\frac{2q_0-r_0}{2M}\right)\left(1+\frac{q_0-r_0}{2M}\right)}{\left[\left(q_0+\frac{\vec{l}^2+\vec{k}^2+q_0^2}{2M}\right)-\frac{|\vec{q}-\vec{l}-\vec{k}|^2}{2M}+i\epsilon\right]\left[\left(q_0-r_0+\frac{\vec{k}^2+(q_0-r_0)^2}{2M}\right)-\frac{|\vec{q}-\vec{r}-\vec{k}|^2}{2M}+i\epsilon\right]}, \tag{36}$$

and

$$\Delta E_{Z2} \doteq \frac{\left(1+\frac{r_0-q_0}{2M}\right)\left(1+\frac{2r_0-q_0}{2M}\right)\left(1+\frac{r_0}{2M}\right)}{\left[\left(r_0-q_0+\frac{\vec{l}^2+(r_0-q_0)^2}{2M}\right)-\frac{|\vec{r}-\vec{l}-\vec{q}|^2}{2M}+i\epsilon\right]\left[\left(r_0+\frac{\vec{k}^2+\vec{l}^2+r_0^2}{2M}\right)-\frac{|\vec{r}-\vec{l}-\vec{k}|^2}{2M}+i\epsilon\right]}. \tag{37}$$

To order m^2/M these reduce to

$$\Delta E_{Z1} \doteq \frac{1}{(q_0+i\epsilon)(q_0-r_0+i\epsilon)}\left(1+\frac{2q_0-r_0}{M}\right)-\frac{1}{2M}\frac{1}{(q_0+i\epsilon)^2}\frac{1}{q_0-r_0+i\epsilon}(\vec{l}^2+\vec{k}^2+q_0^2-|\vec{q}-\vec{l}-\vec{k}|^2)$$
$$-\frac{1}{2M}\frac{1}{q_0+i\epsilon}\frac{1}{(q_0-r_0+i\epsilon)^2}[\vec{k}^2+(q_0-r_0)^2-|\vec{q}-\vec{r}-\vec{k}|^2], \tag{38}$$

and

$$\Delta E_{Z2} \doteq \frac{1}{(r_0-q_0+i\epsilon)(r_0+i\epsilon)}\left(1+\frac{2r_0-q_0}{M}\right)-\frac{1}{2M}\frac{1}{(r_0-q_0+i\epsilon)^2}\frac{1}{r_0+i\epsilon}(\vec{l}^2+(r_0-q_0)^2-|\vec{r}-\vec{l}-\vec{q}|^2)$$
$$-\frac{1}{2M}\frac{1}{r_0-q_0+i\epsilon}\frac{1}{(r_0+i\epsilon)^2}(\vec{l}^2+\vec{k}^2+r_0^2-|\vec{r}-\vec{l}-\vec{k}|^2). \tag{39}$$

We next turn to Y graphs. While reducible, they arise from the correction to the kernel from our formalism, schematically $\delta K = K(S-S_0)K$, where one kernel is the crossed Coulomb ladder and the other a Coulomb exchange. The S_0 term involves a delta function of either q_0 or r_0. This can be canceled by changing the sign of $i\epsilon$ in the nuclear propagator in the graph involving S; that is, we would write

$$\frac{1}{-q_0-\frac{\vec{q}^2}{2M}+i\epsilon} = -\frac{1}{q_0+\frac{\vec{q}^2}{2M}+i\epsilon}-2\pi i\delta\left(q_0+\frac{\vec{q}^2}{2M}\right), \tag{40}$$

with the second term canceling with the S_0 term. After doing this, the Y graphs become

$$\Delta E_{Y1} \doteq \frac{1}{(r_0-q_0+i\epsilon)(-q_0-i\epsilon)}\left(1+\frac{r_0-2q_0}{M}\right)-\frac{1}{2M}$$
$$\times\frac{1}{(r_0-q_0+i\epsilon)^2}\frac{1}{-q_0-i\epsilon}[\vec{l}^2+(r_0-q_0)^2-|\vec{r}-\vec{l}$$
$$-\vec{q}|^2]-\frac{1}{2M}\frac{1}{r_0-q_0+i\epsilon}\frac{1}{(-q_0-i\epsilon)^2}(q_0^2-|\vec{q}|^2), \tag{41}$$

and

$$\Delta E_{Y2} \doteq \frac{1}{(q_0-r_0+i\epsilon)(-r_0-i\epsilon)}\left(1+\frac{q_0-2r_0}{M}\right)$$
$$-\frac{1}{2M}\frac{1}{(-r_0-i\epsilon)^2}\frac{1}{q_0-r_0+i\epsilon}(r_0^2-\vec{r}^2)$$
$$-\frac{1}{2M}\frac{1}{-r_0-i\epsilon}\frac{1}{(q_0-r_0+i\epsilon)^2}[\vec{k}^2+(q_0-r_0)^2$$
$$-|\vec{q}-\vec{r}-\vec{k}|^2]. \tag{42}$$

Finally we need to include the second-order correction to the kernel, with all three kernels being one-Coulomb exchange,

$$\Delta K_2 = K(S-S_0)K(S-S_0)K. \tag{43}$$

This gives rise to the energy shift from the L diagram,

$$\Delta E_L \doteq \frac{1}{(-r_0-i\epsilon)(-q_0-i\epsilon)}\left(1+\frac{-q_0-r_0}{M}\right)$$
$$-\frac{1}{2M}\frac{1}{(-r_0-i\epsilon)^2}\frac{1}{-q_0-i\epsilon}(r_0^2-\vec{r}^2)$$
$$-\frac{1}{2M}\frac{1}{-r_0-i\epsilon}\frac{1}{(-q_0-i\epsilon)^2}(q_0^2-\vec{q}^2). \tag{44}$$

The analysis of the seagull diagrams in Fig. 4 is simpler, as these start in order m^2/M. We note that the transverse

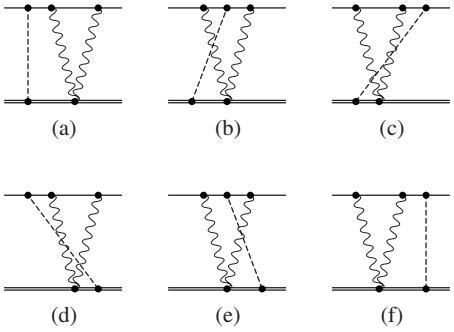

FIG. 4. Seagull two-loop graphs.

photons in this figure are to be replaced with Coulomb photons. A short analysis gives for the irreducible diagrams 4(b)–4(e) the result

$$\Delta E_{\text{seagull-irr}} \doteq -\frac{1}{M}\left(\frac{1}{q_0 - r_0 + i\epsilon} + \frac{1}{r_0 - q_0 + i\epsilon} + \frac{1}{q_0 + i\epsilon} + \frac{1}{r_0 + i\epsilon}\right), \tag{45}$$

and for the reducible diagrams 4(a) and 4(f),

$$\Delta E_{\text{seagull-red}} \doteq \frac{1}{M}\left(\frac{1}{q_0 + i\epsilon} + \frac{1}{r_0 + i\epsilon}\right). \tag{46}$$

This completes our treatment of the three-Coulomb exchange diagrams. All of the nonseagull diagrams have a nonrecoil part, but a short analysis shows that these nonrecoil parts cancel exactly. Also simple to analyze are the seagull diagrams, which sum to

$$\Delta E_{\text{seagull}} \doteq -\frac{1}{M}\left(\frac{1}{q_0 - r_0 + i\epsilon} + \frac{1}{r_0 - q_0 + i\epsilon}\right). \tag{47}$$

If one sums the recoil part of the first line of the expressions for the nonseagull diagrams, one finds the same expression with $-1/M$ replaced with $2/M$. However, the terms in the numerator of the next lines involving q_0^2, r_0^2, and $(q_0-r_0)^2$ sum to the same result as the seagull diagrams, so there is a complete cancellation of such terms. The net result is that one can ignore seagull diagrams so long as the nucleus vertex is taken to be simply $2M$ and the nuclear propagator is proportional to Eq. (A2), for which simplification is crucial for the manipulations given in the Appendix.

The analysis of the remaining recoil terms is complicated because of the presence of eight combinations of $\vec{k}$, $\vec{q}$, $\vec{r}$, and $\vec{l}$ (there could have been ten, but all terms involving $\vec{k}^2$ and $\vec{l}^2$ cancel). Repeated use of the identity

$$\frac{1}{A+B}\left(\frac{1}{A} + \frac{1}{B}\right) = \frac{1}{AB} \tag{48}$$

leads to the exact cancellation of terms proportional to $\vec{q}^2$, $\vec{r}^2$, $\vec{q}\cdot\vec{k}$, and $\vec{l}\cdot\vec{r}$. The remaining terms are all proportional to $\delta(q_0-r_0)$, being specifically

$$\Delta E_{3C} \doteq \frac{2\pi i}{M}\frac{\delta(q_0 - r_0)}{(q_0 + i\epsilon)^2}(\vec{k} - \vec{q})\cdot(\vec{r} - \vec{l}). \tag{49}$$

At this point we restore the complete expression to find

$$\Delta E_{3C} = \frac{i(4\pi Z\alpha)^2}{M(2\pi)^{12}}\int\frac{d^3k d^3q d^3r d^3l}{|\vec{k}-\vec{q}|^2|\vec{r}-\vec{l}|^2}\int\frac{dq_0}{2\pi}\frac{1}{(q_0+i\epsilon)^2} \times(\vec{k}-\vec{q})\cdot(\vec{r}-\vec{l})\bar{\psi}(\vec{l})\gamma_0 S_0(\mathcal{E}_0+q_0;\vec{r})\frac{4\pi Z\alpha\gamma_0}{|\vec{r}-\vec{q}|^2} \times S_0(\mathcal{E}_0+q_0;\vec{q})\gamma_0\psi(\vec{k}). \tag{50}$$

As done in our previous paper [1], we recognize the one-Coulomb part of the Dirac-Coulomb propagator. Restoring the entire propagator, the rigorous justification of which will be given in the Appendix, we find

$$\Delta E_{\text{all-}C} = -\frac{i(4\pi Z\alpha)^2}{M(2\pi)^{12}}\int\frac{d^3k d^3q d^3r d^3l}{|\vec{k}-\vec{q}|^2|\vec{r}-\vec{l}|^2}\int\frac{dq_0}{2\pi} \times\frac{(\vec{k}-\vec{q})\cdot(\vec{r}-\vec{l})}{(q_0+i\epsilon)^2}\bar{\psi}(\vec{l})\gamma_0 S_F(\mathcal{E}_0+q_0;\vec{r},\vec{q})\gamma_0\psi(\vec{k}). \tag{51}$$

The numerical evaluation of this term will be described below. A check on the calculation is provided by replacing $S_F(\mathcal{E}_0+q_0;\vec{r},\vec{q})$ with the free propagator, which gives results in good agreement with the one-loop calculations described in the previous section.

B. Two-transverse–one-Coulomb terms

There are six diagrams that contribute in this order, shown in Fig. 4. We route the momentum in the same way, but of course the structure is now more complicated. The calculation breaks into three parts, each of which has a different kind of non-nuclear structure. Because the contributions are of the order of interest, one can immediately make approximations on the nuclear denominators, keeping only the first term in Eq. (34). A short analysis shows that graphs 4(a) and 4(d) combine to give ΔE_{TT} of Eq. (30), a contribution that is removed by the formalism. Similarly the combination of graphs 4(c) and 4(f) is subtracted away by the formalism. However, graphs 4(b) and 4(e), which have the same non-nuclear structure, have nuclear denominators that give a $\delta(q_0-r_0)$, and lead to

$$\Delta E_{TTC} = -\frac{(4\pi Z\alpha)^2 i}{M}\int\frac{d^3k d^3r d^3q d^3l}{(2\pi)^{12}}\int\frac{dq_0}{2\pi}D_{ik}(q_1)D_{jk}(q_2) \times\bar{\psi}(\vec{l})\gamma_i S_0(\mathcal{E}_0+q_0;\vec{r})\frac{4\pi Z\alpha\gamma_0}{|\vec{r}-\vec{q}|^2}S_0(\mathcal{E}_0+q_0;\vec{q})\gamma_j\psi(\vec{k}), \tag{52}$$

with $\vec{q}_1=\vec{r}-\vec{l}$ and $\vec{q}_2=\vec{q}-\vec{k}$ and $q_{10}=q_{20}=q_0$. We again recognize $S_F^{(1)}$ appearing, and replacing it with S_F gives the complete contribution of two-transverse photon terms,

$$\Delta E_{TT\ \text{all-}C} = \frac{(4\pi Z\alpha)^2 i}{M}\int\frac{dq_0}{2\pi}\int\frac{d^3k d^3r d^3q d^3l}{(2\pi)^{12}} \times D_{ik}(q_1)D_{jk}(q_2)\bar{\psi}(\vec{l})\gamma_i S_F(\mathcal{E}_0+q_0,\vec{r},\vec{q})\gamma_j\psi(\vec{k}). \tag{53}$$

We note that this is the explicit form of the one-Coulomb part of the complete transverse seagull contribution presented in Eq. (A101). A check on the calculation is provided by coding the exact expression, but then replacing S_F with S_0, which must give the *TT* graph calculated in the previous section.

C. One-transverse–two-Coulomb terms

We treated corrections where one transverse photon is accompanied by one or more Coulomb photons in Ref. [1] by first considering one-transverse–two-Coulomb photon exchange diagrams. We showed that they involved the one-potential part of the Dirac-Coulomb propagator, Eq. (31), then replaced S_{1C} with S_F, and, after using a spectral representation found

$$\Delta E_{1T\ \text{all-}C} = -\frac{(4\pi Z\alpha)^2}{M}\int\frac{d^3k}{(2\pi)^3}\frac{1}{k^2}\int\frac{d^3l}{(2\pi)^3}\int\frac{d^3p d^3p'}{(2\pi)^6} \times(p-l)_j\left(\delta_{ij}-\frac{k_i k_j}{\vec{k}^2}\right)\frac{1}{|\vec{l}-\vec{p}|^2} \times\sum_m\frac{\bar{\psi}(\vec{p}\,')\gamma_i\psi_m(\vec{p}\,'+\vec{k})\bar{\psi}_m(\vec{l})\gamma_0\psi(\vec{p})}{\mathcal{E}_0-\mathcal{E}_{0m}-k}. \tag{54}$$

(We note that a factor of two has been inserted in Eq. (68) of Ref. [1], where only one of a pair of graphs was analyzed.) However, while this formula is correct when m is a positive energy state, more care is needed when it is a negative energy state. To properly include these states we carry out an analysis of the six graphs of Fig. 3, with the understanding that each graph has three contributions, depending on which of the three photons changes from Coulomb to transverse. (The seagull diagrams of Fig. 4, which in this case have the transverse and Coulomb photons switched, are of higher order in m/M.) A short analysis shows that when that transverse photon connects in the middle of the electron line a set of cancellations between the six diagrams gives a vanishing result. When the photon that first encounters the incoming electron line is transverse, the cancellations between the six diagrams are incomplete, leaving the structure

$$\Delta E_{1TA} = \frac{(4\pi Z\alpha)^3}{2M}\int\frac{d^3k d^3l}{(2\pi)^6}\int\frac{d^4q}{(2\pi)^4}\int\frac{d^4r}{(2\pi)^4}\frac{D_{ij}(q-k)}{|\vec{r}-\vec{l}|^2|\vec{r}-\vec{q}|^2} \times\bar{\psi}(\vec{l})\gamma_0 S_0(\mathcal{E}_0+r_0;\vec{r})\gamma_0 S_0(\mathcal{E}_0+q_0;\vec{q})\gamma_i \times\psi(\vec{k})2\pi i\delta(q_0-r_0)\frac{2(l-r)_j}{q_0+i\epsilon}. \tag{55}$$

When the photon that connects with the outgoing electron line is transverse the above contribution is effectively doubled, giving a total effect of

$$\Delta E_{1TAC} = -\frac{(4\pi Z\alpha)^2 i}{M}\int\frac{d^3k d^3l}{(2\pi)^3}\int\frac{d^3q}{(2\pi)^3}\int\frac{dq_0}{2\pi}\int\frac{d^3r}{(2\pi)^3} \times\frac{D_{ij}(q-k)}{|\vec{r}-\vec{l}|^2}\bar{\psi}(\vec{l})\gamma_0 S_{1C}(\mathcal{E}_0+q_0,\vec{r},\vec{q})\gamma_i\psi(\vec{k})\frac{2(l-r)_j}{q_0+i\epsilon}. \tag{56}$$

Now restoring the complete Dirac-Coulomb propagator in the above and using its spectral representation, we find the all-orders expression

$$\Delta E_{1T\ \text{all-}C} = -\frac{(4\pi Z\alpha)^2 i}{M}\sum_m\int\frac{d^3k d^3l}{(2\pi)^6}\int\frac{d^3q}{(2\pi)^3} \times\int\frac{dq_0}{2\pi}\int\frac{d^3r}{(2\pi)^3}\frac{D_{ij}(q-k)}{|\vec{r}-\vec{l}|^2} \times\frac{\psi^\dagger(\vec{l})\psi_m(\vec{r})\psi_m^\dagger(\vec{q})\alpha_i\psi(\vec{k})}{\mathcal{E}_0+q_0-\mathcal{E}_{0m}(1-i\delta)}\frac{2(l-r)_j}{q_0+i\epsilon}. \tag{57}$$

If the sum over m is restricted to positive energy states, carrying out the q_0 integration by closing above encloses only the pole from the transverse photon propagator, and reproduces our previous result after variable changes. However, if one sums over negative energy states, an extra pole will be encircled. This can be accounted for by simply making a simple denominator substitution described in the next section.

VI. NUMERICAL EVALUATION OF ALL-ORDERS TERMS

We begin the evaluation of higher-order terms with the all-Coulomb result. Using the spectral representation of S_F, Eq. (2) allows us to write Eq. (51) as

$$\Delta E_{\text{all-}C} = -\frac{i(4\pi Z\alpha)^2}{M}\sum_m\int\frac{dq_0}{2\pi} \times\frac{1}{(q_0+i\epsilon)^2[\mathcal{E}_{0v}+q_0-\mathcal{E}_{0m}(1-i\delta)]}\vec{A}_m\cdot\vec{B}_m, \tag{58}$$

where

$$\vec{A}_m = \int\frac{d^3l d^3r}{(2\pi)^6|\vec{l}-\vec{r}|^2}(\vec{r}-\vec{l})\psi_v^\dagger(\vec{l})\psi_m(\vec{r}), \tag{59}$$

and

$$\vec{B}_m = \int\frac{d^3q d^3k}{(2\pi)^6|\vec{q}-\vec{k}|^2}(\vec{k}-\vec{q})\psi_m^\dagger(\vec{q})\psi_v(\vec{k}). \tag{60}$$

The integration over q_0 vanishes for positive energy states, giving

$$\Delta E_{\text{all-}C} = \frac{(4\pi Z\alpha)^2}{M}\sum_m{}'\frac{\vec{A}_m\cdot\vec{B}_m}{(\mathcal{E}_{0v}-\mathcal{E}_{0m})^2}, \tag{61}$$

where the prime indicates only negative energy states are summed over. The energy denominator is canceled once we use

$$\vec{A}_m = \frac{1}{4\pi Z\alpha}(\mathcal{E}_{0m} - \mathcal{E}_{0v})\langle v|\vec{p}|m\rangle, \tag{62}$$

and

$$\vec{B}_m = \frac{1}{4\pi Z\alpha}(\mathcal{E}_{0v} - \mathcal{E}_{0m})\langle m|\vec{p}|v\rangle, \tag{63}$$

which follow from the use of

$$[\vec{p},H] = -\frac{iZ\alpha\hat{r}}{r^2}. \tag{64}$$

The final form of the all-Coulomb result is then quite simple,

$$\Delta E_{\text{all-}C} = -\frac{1}{M}\sum_m{}' \langle v|\vec{p}|m\rangle \cdot \langle m|\vec{p}|v\rangle. \tag{65}$$

If we denote $\Sigma' |m\rangle\langle m|$ as Λ_-, this is the same as the more rigorously derived Eq. (A105).

The matrix elements of $\vec{p}$ between Dirac wave functions require some care, but the end result always involves integrals over the upper and lower components of the form

$$I \equiv \int dr\left[g_m(r)\left(\frac{dg_v(r)}{dr} + \frac{A}{r}g_v(r)\right) + f_m(r)\left(\frac{df_v(r)}{dr} + \frac{B}{r}f_v(r)\right)\right]. \tag{66}$$

A Clebsch-Gordon factor C gives an overall contribution of $-CI^2/M$. When $\kappa_v=-1$ the values of $\{A,B,C\}$ are $\{-1,1,1/3\}$ for $\kappa_m=1$, and $\{-1,-2,2/3\}$ for $\kappa_m=-2$. When $\kappa_v=1$ the values are $\{1,-1,1/3\}$ for $\kappa_m=-1$, and $\{-2,-1,2/3\}$ for $\kappa_m=2$. For $\kappa_v=-2$ there are three possibilities, with $\{A,B,C\}$ being $\{1,2,1/3\}$ for $\kappa_m=-1$, $\{-2,2,1/15\}$ for $\kappa_m=2$, and $\{-2,-3,3/5\}$ for $\kappa_m=-3$. When $\kappa_v=2$ they are $\{2,1,1/3\}$ for $\kappa_m=1$, $\{2,-2,1/15\}$ for $\kappa_m=-2$, and $\{-3,-2,3/5\}$ for $\kappa_m=3$. Finally, when $\kappa_v=-3$ the values are $\{2,3,2/5\}$ for $\kappa_m=-2$, $\{-3,3,1/35\}$ for $\kappa_m=3$, and $\{-3,-4,4/7\}$ for $\kappa_m=-4$. The constants can be obtained by either directly integrating over solid angles together with averaging over magnetic quantum numbers or else by Racah algebra methods. The radial functions $g(r)$ and $f(r)$ come from the coordinate space representation of the wave function

$$\psi(\vec{r}) = \frac{(mZ\alpha)^{3/2}}{r}\begin{pmatrix} ig(r)\chi_{\kappa\mu}(\hat{r}) \\ f(r)\chi_{-\kappa\mu}(\hat{r}) \end{pmatrix}, \tag{67}$$

where r is understood to be in atomic units. We use finite basis set techniques [9,10] to evaluate this term. When one creates a finite basis set for a given κ value, one typically makes $n \approx 100$ positive energy states and 100 negative states in a cavity of radius R, where R is chosen to be much larger than the ion. The first few positive energy states are very close to the first bound states of the ion, but we sum only over the 100 negative energy states in order to evaluate the all-Coulomb term. We vary the number of states n and the radius R to test the accuracy of the basis set.

Because we have already calculated the one-loop Coulomb exchange result, we subtract this term from the calculation described above, and present the difference in the seventh column of Table II. This is done "by hand" rather than working with free propagators represented with spline basis sets, as we will do for the one- and two-transverse photon terms. The reason for this is that the manipulation used to derive the simple form above mixes orders of perturbation theory.

We next turn to the one-transverse photon correction. The coordinate space form of Eq. (54) is

$$\Delta E_{1T\ \text{all-}C} = \frac{4\pi i(Z\alpha)^2}{M}\int \frac{d^3k}{(2\pi)^3}\frac{1}{k^2}\left(\delta_{ij} - \frac{k_i k_j}{k^2}\right) \times \sum_m \frac{A_i(vm)B_j(mv)}{\mathcal{E}_{0v} - \mathcal{E}_{0m} - k}, \tag{68}$$

where

$$A_i(vm) = \int d^3y e^{i\vec{k}\cdot\vec{y}}\psi_v^\dagger(\vec{y})\alpha_i\psi_m(\vec{y}), \tag{69}$$

and

$$B_j(mv) = \int d^3x \frac{x_j}{x^3}\psi_m^\dagger(\vec{x})\psi_v(\vec{x}). \tag{70}$$

As discussed above, this comes from taking the transverse photon pole in Eq. (57), valid only if the intermediate state m is positive energy. If it is negative energy, an extra term is present that can be accounted for by making the substitution

$$\frac{1}{\mathcal{E}_{0v} - \mathcal{E}_{0m} - k} \to \frac{(\mathcal{E}_{0v} - \mathcal{E}_{0m} + 2k)}{(\mathcal{E}_{0v} - \mathcal{E}_{0m})(\mathcal{E}_{0v} - \mathcal{E}_{0m} + k)}. \tag{71}$$

An angular momentum analysis leads to the expression

$$\Delta E_{1T\ \text{all-}C} = \frac{4(Z\alpha)^2}{\pi M\sqrt{3}}\sum_m \frac{1}{D_{vm}}\frac{C_1^2(vm)}{2j_v+1} \times \int_0^\infty \frac{dx}{x^2}R_{mv}(x)\int_0^\infty dy\int_0^\infty dk \times \left[j_0(ky)Q_{vm}^1(y) - \frac{1}{\sqrt{2}}j_2(ky)P_{vm}^1(y)\right], \tag{72}$$

where

$$C_l(ab) \equiv (-1)^{j_a+1/2}\sqrt{(2j_a+1)(2j_b+1)}\begin{pmatrix} l & j_a & j_b \\ 0 & -\frac{1}{2} & \frac{1}{2} \end{pmatrix}, \tag{73}$$

$$R_{vm}(x) \equiv g_v(x)g_m(x) + f_v(x)f_m(x), \tag{74}$$

$$Q_{vm}^J(x) \equiv \sqrt{\frac{J}{2J+1}}\left[f_v(x)g_m(x) - g_v(x)f_m(x) + \frac{\kappa_v - \kappa_m}{J}[g_v(x)f_m(x) + f_v(x)g_m(x)]\right], \tag{75}$$

and

$$P^J_{vm}(x) \equiv \sqrt{\frac{J+1}{2J+1}}\left[-f_v(x)g_m(x)+g_v(x)f_m(x) + \frac{\kappa_v-\kappa_m}{J+1}[g_v(x)f_m(x)+f_v(x)g_m(x)]\right]. \quad (76)$$

Here $C_l(ab)$ is understood to vanish if $l+l_a+l_b$ is odd, and D_{vm} is the denominator defined in Eq. (71).

There are two ways to evaluate the integral of k. As it stands, the integral is undefined for excited states, because the denominator can vanish. However, since in this paper we are interested only in the real part of the integral, we can evaluate the principal part of the integral. This can easily be done when using Gaussian integration by integrating symmetrically about the zeros of the denominator. However, using this method requires a very large number of Gaussian points for large values of k, as the spherical Bessel functions oscillate rapidly. A more numerically stable procedure comes from not using Cauchy's theorem, but instead carrying out the Wick rotation $q_0 \to i\omega$. This procedure, in general, encircles poles, so that two expressions must be evaluated: a pole term, which has both real and imaginary parts, and an integration along the imaginary axis, which is purely real. In this case the high energy behavior involves damped exponentials, and is easier to control. Good agreement between the two methods was found. We will treat the imaginary parts, which give recoil corrections to decay rates, in a separate paper. A check on the calculation is afforded by replacing the propagator with a free propagator and making sure the fifth column of Table II is reproduced, after which the difference is tabulated in the eighth column.

Finally, we consider the two-transverse photon seagull term, Eq. (53). While the transverse photon propagator is simple in momentum space, its coordinate space form is more complicated, specifically

$$D_{ij}(k) = -\frac{1}{4\pi}\int d^3x e^{-i\vec{k}\cdot\vec{x}}\left[A(k_0,x)\delta_{ij}+B(k_0,x)\frac{x_i x_j}{x^2}\right], \quad (77)$$

with $x=|\vec{x}|$,

$$A(k_0,x) = \frac{1}{k_0^2 x^3} + \frac{e^{ik_0x}}{x}\left(1+\frac{ik_0x-1}{k_0^2x^2}\right), \quad (78)$$

and

$$B(k_0,x) = -\frac{3}{k_0^2x^3} + \frac{e^{ik_0x}}{k_0^2x^3}(3-3ik_0x-k_0^2x^2). \quad (79)$$

In terms of these functions we can write

$$\Delta E_{TT\ \text{all-}C} = \frac{i(Z\alpha)^2}{M}\sum_m \int \frac{d^3x d^3y}{(2\pi)^3}\int \frac{dq_0}{2\pi} \times \frac{\psi^\dagger_v(\vec{x})\alpha_i\psi_m(\vec{x})\psi^\dagger_m(\vec{y})\alpha_j\psi(\vec{y})}{\mathcal{E}_{0v}+q_0-\mathcal{E}_{0m}(1-i\delta)} \times\left(A(q_0,x)\delta_{ik}+B(q_0,x)\frac{x_ix_k}{x^2}\right) \times\left(A(q_0,y)\delta_{jk}+B(q_0,y)\frac{y_jy_k}{y^2}\right). \quad (80)$$

We break this expression up into a term with two factors of B,

$$\Delta E_{TT1} = -\frac{i(Z\alpha)^2}{8\pi^3M}\sum_m \frac{C_1^2(vm)}{2j_v+1}\int\frac{dq_0}{2\pi}\int_0^\infty dx \times\int_0^\infty dy \frac{B(q_0,x)B(q_0,y)}{\mathcal{E}_{0v}+q_0-\mathcal{E}_{0m}}S_{vm}(x)S_{mv}(y), \quad (81)$$

a term with two factors of A,

$$\Delta E_{TT2} = -\frac{3i(Z\alpha)^2}{8\pi^3M}\sum_m \frac{C_1^2(vm)}{2j_v+1}\int\frac{dq_0}{2\pi}\int_0^\infty dx \times\int_0^\infty dy \frac{A(q_0,x)A(q_0,y)}{\mathcal{E}_{0v}+q_0-\mathcal{E}_{0m}}Q^1_{vm}(x)Q^1_{mv}(y), \quad (82)$$

and terms with one A and one B factor,

$$\Delta E_{TT34} = \frac{\sqrt{3}i(Z\alpha)^2}{8\pi^3M}\sum_m \frac{C_1^2(vm)}{2j_v+1}\int\frac{dq_0}{2\pi}\int_0^\infty dx \times\int_0^\infty dy \frac{A(q_0,x)B(q_0,y)}{\mathcal{E}_{0v}+q_0-\mathcal{E}_{0m}}Q^1_{vm}(x)S_{mv}(y) + \frac{\sqrt{3}i(Z\alpha)^2}{8\pi^3M} \times\sum_m \frac{C_1^2(vm)}{2j_v+1}\int\frac{dq_0}{2\pi}\int_0^\infty dx\int_0^\infty dy \frac{B(q_0,x)A(q_0,y)}{\mathcal{E}_{0v}+q_0-\mathcal{E}_{0m}} \times S_{vm}(x)Q^1_{mv}(y), \quad (83)$$

where

$$S_{mv}(x) \equiv g_m(x)f_v(y)-f_m(x)g_v(y). \quad (84)$$

We perform a Wick rotation $q_0 \to i\omega$ to evaluate these expressions, which again leads to both an ω integral performed with Gaussian integration and a set of terms associated with encircling poles. The difference of the full expression with the one-loop result, again used as a check on the coding by making sure the replacement $S_F \to S_0$ reproduces column six, is presented in the ninth column of Table II, and the sum is given in the last column. Table III gives the sum for the isolectronic sequence.

VII. DISCUSSION AND CONCLUSIONS

There are several features of the calculation presented above that we wish to highlight. They are error estimates, comparison with low-Z analytic results, comparison with other calculations, and finally, the role of the calculation for lithiumlike and sodiumlike ions.

With regard to error, while the small overall size of recoil means that high accuracy in the calculations is not vital, interesting issues involving basis sets arose that we wish to discuss. Most of the numbers in the tables came from using 100 basis sets (which means 100 positive energy and 100 negative energy states for each value of κ). In most applications of finite basis sets this gives results of high accuracy. In addition, the cavity radius in which the basis sets were formed was chosen to be $R=100/Z$, again usually a choice that gives very precise results. In fact, for the middle range

TABLE III. $R(n,\kappa,Z\alpha)$ for all $n=1,2$, and 3 states of hydrogenic ions.

Z	$1s$	$2s$	$2p_{1/2}$	$2p_{3/2}$	$3s$	$3p_{1/2}$	$3p_{3/2}$	$3d_{3/2}$	$3d_{5/2}$
1	1.7248	0.2441	−0.0119	−0.0120	0.0743	−0.0030	−0.0033	−0.0008	−0.0007
5	1.3693	0.2007	−0.0102	−0.0108	0.0615	−0.0026	−0.0028	−0.0006	−0.0007
10	1.2077	0.1818	−0.0080	−0.0095	0.0559	−0.0019	−0.0025	−0.0005	−0.0007
20	1.0484	0.1647	−0.0032	−0.0069	0.0511	−0.0002	−0.0016	−0.0004	−0.0005
30	0.9687	0.1589	0.0020	−0.0044	0.0495	0.0015	−0.0007	−0.0003	−0.0004
40	0.9316	0.1595	0.0076	−0.0021	0.0498	0.0035	0.0001	−0.0002	−0.0002
50	0.9273	0.1664	0.0142	0.0002	0.0520	0.0058	0.0007	0.0000	−0.0002
60	0.9568	0.1798	0.0223	0.0024	0.0563	0.0087	0.0015	0.0000	−0.0001
70	1.0290	0.2032	0.0330	0.0045	0.0633	0.0124	0.0023	0.0004	0.0000
80	1.1683	0.2616	0.0484	0.0056	0.0754	0.0178	0.0032	0.0005	0.0001
83	1.2305	0.2598	0.0545	0.0071	0.0806	0.0199	0.0034	0.0006	0.0001
90	1.4363	0.3146	0.0733	0.0075	0.0973	0.0264	0.0040	0.0007	0.0003
92	1.5174	0.3361	0.0803	0.0079	0.1037	0.0288	0.0041	0.0007	0.0003
100	2.0217	0.4684	0.1221	0.0073	0.1432	0.0254	0.0048	0.0009	0.0004

of Z, between 10 and 80, the basis set worked very well. The problems came from low Z, between 1 and 10, and high Z, between 80 and 100. The primary source of error in these two cases came from the fact that the results changed as the cavity radius was increased. A secondary source of error was the use of 100 basis sets, as going up to 500 in steps of 100 led to changes, but these were smaller than the error associated with the cavity radius. The problem was less severe at high Z, where, for example, the largest change in going from a basis set of size 100 to 400 was in $Z=92$ $3p_{3/2}$, which shifted by 0.000 35 atomic units, or 0.0097 eV. However, at lower Z, particularly $Z=1$ and 5, we were unable to fully control the dependence of the result on cavity radius, finding independence of the radius only at unphysically large values. The results were stable only at the 0.01 level, which made the fits to analytic forms, discussed below, difficult.

Turning now to the comparison with the known $Z\alpha$ expansion, we must first deal with the convention that terms of order $m^2/M(Z\alpha)^6$ are presented in the form

$$E_R = \frac{m^2(Z\alpha)^6}{Mn^3} D_{60}(n,l,Z\alpha), \tag{85}$$

where the current state of knowledge of the function D_{60} will be described below. However, these calculations include lower order recoil effects through the equation

$$E = m + m_r[f(n,j) - 1] - \frac{m_r^2}{2M}[f(n,j) - 1]^2$$
$$= m + m[f(n,j) - 1] + \frac{m^2 - \mathcal{E}^2}{2M}, \tag{86}$$

where the second equality follows from using $\mathcal{E}=mf(n,j)$ and dropping terms of order m^3/M^2. While our definition, Eq. (20), differs from this, the difference comes from the sum of ΔE_A and ΔE_{1T}, so in the following we do not include those terms, though we note that at low Z they have the form

$$\delta E_{\text{formalism}} = -\frac{m^2(Z\alpha)^6}{8Mn^6(j+1/2)^3}[4(j+1/2)^3 - 8n(j+1/2)^2 + 3n^2(j+1/2) + n^3]. \tag{87}$$

For s states D_{60} is known to be

$$D_{60}(n,0,Z\alpha) = 4\ln 2 - \frac{7}{2} - \frac{11}{15\pi}(Z\alpha)\ln^2(Z\alpha), \tag{88}$$

and for non-s states

$$D_{60}(n,l\neq 0,0) = \left[3 - \frac{l(l+1)}{n^2}\right]\frac{2}{(4l^2-1)(2l+3)}. \tag{89}$$

We note that the logarithmic term, calculated by two groups [18,19], was given incorrectly in the Appendix of our previous paper [1].

At this point we can now compare our low-Z results with previous calculations and the perturbative expansion. We reproduce in the fifth column of Table IV values of R for $Z=5$, 10, and 20 for the nine states considered in this paper with the exclusion of ΔE_A and ΔE_{1T}, denoting that modification by $\tilde{R}$. In the second column we present the Salpeter correction,

$$E_S = \frac{m^2(Z\alpha)^5}{\pi Mn^3}\left[-\frac{2}{3}\delta_{l0}\ln Z\alpha - \frac{8}{3}\ln k_0(n,l) - \frac{1}{9}\delta_{l0} - \frac{7}{3}a_n\right], \tag{90}$$

where the values of a_n for the nine states considered in this paper are $-2\ln 2-3$, $-9/2$, $1/6$, $1/6$, $2\ln(3/2)-16/3$, $1/6$, $1/6$, $1/30$, and $1/30$. The Bethe logarithms needed are 2.984 13, 2.811 77, −0.030 02, −0.030 02, 2.767 66, −0.038 19, −0.038 19, −0.005 23, and −0.005 23 [16]. Clear deviations from our results are seen. Inclusion of D_{60}, done in the following column, improves the agreement significantly for non-s states, but higher-order terms beyond the squared logarithmic term included in D_{60} are clearly present for s states. For that case we have done a simple fit, adding a

TABLE IV. Comparison of perturbative expansions in $Z\alpha$ with low-Z values of $\tilde{R}$ and Refs. [11,12].

State, Z	S	$S+D_{60}$	$S+D_{60}$+H.O.	$\tilde{R}$	Artemyev *et al.*
$1s,Z=5$	1.3920	1.3621	1.3696	1.3693	1.3698
$1s,Z=10$	1.2449	1.1833	1.2077	1.2077	1.2080
$1s,Z=20$	1.0978	0.9732	1.0484	1.0484	1.0485
$2s,Z=5$	0.2028	0.1991	0.2003	0.2001	0.2003
$2s,Z=10$	0.1845	0.1768	0.1806	0.1806	0.1806
$2s,Z=20$	0.1661	0.1505	0.1624	0.1624	0.1624
$2p_{1/2},Z=5$	−0.0123	−0.0108		−0.0107	−0.0107
$2p_{1/2},Z=10$	−0.0123	−0.0093		−0.0091	−0.0091
$2p_{1/2},Z=20$	−0.0123	−0.0062		−0.0055	−0.0055
$2p_{3/2},Z=5$	−0.0123	−0.0108		−0.0108	−0.0108
$2p_{3/2},Z=10$	−0.0123	−0.0093		−0.0095	−0.0095
$2p_{3/2},Z=20$	−0.0123	−0.0062		−0.0069	−0.0069
$3s,Z=5$	0.0621	0.0610	0.0613	0.0613	
$3s,Z=10$	0.0567	0.0544	0.0555	0.0555	
$3s,Z=20$	0.0512	0.0466	0.0502	0.0502	
$3p_{1/2},Z=5$	−0.0034	−0.0029		−0.0028	
$3p_{1/2},Z=10$	−0.0034	−0.0024		−0.0023	
$3p_{1/2},Z=20$	−0.0034	−0.0014		−0.0011	
$3p_{3/2},Z=5$	−0.0034	−0.0029		−0.0029	
$3p_{3/2},Z=10$	−0.0034	−0.0024		−0.0025	
$3p_{3/2},Z=20$	−0.0034	−0.0014		−0.0016	
$3d_{3/2},Z=5$	−0.0008	−0.0007		−0.0006	
$3d_{3/2},Z=10$	−0.0008	−0.0006		−0.0006	
$3d_{3/2},Z=20$	−0.0008	−0.0005		−0.0005	
$3d_{5/2},Z=5$	−0.0008	−0.0007		−0.0007	
$3d_{5/2},Z=10$	−0.0008	−0.0006		−0.0007	
$3d_{5/2},Z=20$	−0.0008	−0.0005		−0.0005	

form $m^2/M(Z\alpha)^7[A+B\ln Z\alpha]$, referred to in the table as "H.O." for higher order, which is seen to give good agreement. In the final column we present the results of Shabaev's group for $n=1$ and $n=2$ states, and note we have excellent agreement except for the $Z=5$ $1s$ case, where the numerical difficulties mentioned above most likely account for the small discrepancy.

The values of A for $n=1$, 2, and 3 are 0.6076, 0.1281, and 0.0646, and the values of B are −1.519, −0.224, and −0.054, respectively. The logarithmic terms behave roughly as $1/n^3$, as expected, but the constant terms deviate from this pattern, probably because of the roughness of our fit, but possibly because of state dependence of these constants, which have not as yet been treated analytically. While not shown in the table, we note that our fit for $Z=30$ continues to give close agreement.

We finally discuss the role of this calculation for highly charged ions with $Z=83$ and $Z=92$. While these are many-electron ions, a rapidly convergent perturbation expansion can be formed starting with a Slater determinant of a heliumlike core and a valence electron for lithiumlike ions, and a neonlike core with a valence electron for sodiumlike ions. Particularly for lithiumlike ions the interelectron interaction can be ignored in lowest order, so that each electron is in one of the hydrogenic orbitals treated in this paper. In this case the recoil corrections calculated here sum linearly. Because the experiments measure differences between states with the same core but different valence states, the contribution from the core cancels out. Using the values of $R(Z,\kappa,Z\alpha)$ from the tables along with the definition Eq. (20), we find the contributions to the states of interest for $Z=83$ and $Z=92$ shown in Table V. For the $2p_{3/2}$-$2s$ transition in lithiumlike bismuth this contributes −0.033 eV, and for the $2p_{1/2}$-$2s$

TABLE V. Total one-electron recoil contributions to $Z=83$ and $Z=92$ states in eV.

State	$Z=83$	$Z=92$
$2s$	0.095	0.127
$2p_{1/2}$	0.073	0.086
$2p_{3/2}$	0.062	0.067
$3s$	0.038	0.049
$3p_{1/2}$	0.031	0.036
$3p_{3/2}$	0.028	0.031

transition in lithiumlike uranium −0.041 eV. These numbers are in good agreement with Artemyev *et al.* For the sodiumlike uranium transition $3p_{3/2}$-$3s_{1/2}$, the one electron recoil result is −0.018 eV.

These contributions are much smaller than the nonrecoil part of the calculation, but are of the order of the recently calculated two-loop Lamb shift [17]. However, another recoil correction must also be considered, that of mass polarization. Our formalism is based on the two-body problem, and does not immediately apply to multielectron atoms and ions. While the Artemyev *et al.* [11,12] calculations include both one-electron and many-electron recoil contributions, one of the purposes of this research has been to provide an independent derivation of their results. We have done so in this paper for the one-electron case, and are at present attempting to generalize the Bethe-Salpeter approach so as to rederive their formulas for the many-electron case. Independently of this research effort, numerical evaluation of these formulas using different numerical techniques can be done, and we are at present, in collaboration with K. T. Cheng, carrying out these calculations.

ACKNOWLEDGMENTS

The work of J.S. and S.M. was supported in part by NSF Grant No. PHY-0451842. Useful conversations with K. T. Cheng and K. Pachucki are gratefully acknowledged. G.S.A. acknowledges the hospitality of the Aspen Center for Physics, where part of this work was done.

APPENDIX: DERIVATION OF THE FORMULA FOR THE RECOIL CORRECTION TO ALL ORDERS

1. Introduction

The purpose of this Appendix is to derive an expression for the first-order recoil correction to the energy of a two-body bound state to all orders in $Z\alpha$, giving the details of the derivation. We consider two-body bound states in which one body of mass m (the "electron") is relatively light, and the other of mass M with $M \gg m$ (the "nucleus") is heavy. The two are charged, with charges $-e$ and Ze, and interact electrodynamically. We intend to study energy levels for this system. In the lowest order of approximation in m/M, the heavy particle is stationary and can be considered to be a fixed center of force. The relevant equation in this case is the Dirac equation for the mass m particle moving in the Coulombic potential of the mass M particle. In this work we are interested in the first-order recoil corrections to the energy, which will depend on the masses as m^2/M.

In the usual approach to the calculation of energies of QED bound states, a perturbative scheme is set up in the small parameter α, or here $Z\alpha$. This kind of approach will not work for us since we intend to work at high Z where $Z\alpha$ is not small. Following Braun [7] and Shabaev [8], we reorganize the perturbative scheme so that m/M is the small parameter, and show how to sum the resulting series at $O(1)$ and $O(m/M)$ to all orders in $Z\alpha$. The complete result at $O(m/M)$ was first obtained by Shabaev [8]. It was also obtained using a different approach by Pachucki and Grotch [20]. Our discussion follows that of Shabaev [8] since we want to maintain close contact with a graphical approach. Shabaev's derivation is quite abbreviated, and we fill in many of the missing steps. Finally, we derive Yelkhovsky's simplified form for the $O(m/M)$ correction [21].

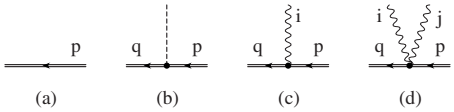

FIG. 5. Diagram parts for the NRQED description of the nucleus. The free propagator is represented in (a). The basic Coulomb interaction appears in (b). The transverse dipole and transverse seagull interactions are shown in (c) and (d).

Since we are only interested in corrections of order $1/M$, we can use nonrelativistic QED (NRQED) to describe the field theory of the nucleus [22]. This simplifies the calculation tremendously, since the NRQED propagator has but one pole (the "particle" pole), and to order $1/M$ for a spinless nucleus there are only three interactions: the instantaneous Coulomb vertex, the "dipole" vertex involving a single transverse photon, and the transverse seagull involving two transverse photons.

The nucleus has a large mass relative to the electron and moves nonrelativistically. In order to calculate the first recoil corrections (proportional to m/M) we must take this motion into account, but only to first order. It is natural then to describe the nucleus using NRQED, even while the electron motion is considered using the full QED. The NRQED Lagrangian is [23]

$$\mathcal{L}_N = \phi^\dagger \left\{ iD_t + \frac{\vec{D}^2}{2M} + \cdots \right\} \phi, \tag{A1}$$

where $D_t = \partial_t - iZeA^0$ and $\vec{D} = \vec{\partial} + iZe\vec{A}$. In our case the nucleus field is described by the spin-0 field ϕ. The propagator and interactions are shown in Fig. 5. The corresponding Feynman rules are

$$\frac{i}{(p_0 - M) - \dfrac{\vec{p}^2}{2M} + i\epsilon}, \tag{A2}$$

for the NRQED nuclear propagator of Fig. 5(a), and

$$iZe, \quad iZe\frac{(q+p)^i}{2M}, \quad -i(Ze)^2\frac{\delta_{ij}}{2M} \tag{A3}$$

for the Coulomb, transverse dipole, and transverse seagull interactions of Figs. 5(b)–5(d). Note that the NRQED propagator depends on the nonrelativistic energy $p_0 - M$ running through the nucleus line, not the total energy p_0. The electron and photon propagation factors have their standard (Coulomb gauge) QED forms as follows:

$$\frac{i}{\gamma p - m + i\epsilon} \tag{A4}$$

for the electron, and

$$iD_{00}(k) = \frac{i}{\vec{k}^2 + i\epsilon}, \quad iD_{ij}(k) = \frac{i}{k^2 + i\epsilon}\left(\delta_{ij} - \frac{k_i k_j}{\vec{k}^2}\right) \tag{A5}$$

for the Coulomb and transverse photons. The electron-photon vertex Feynman rule is the usual $-ie\gamma^\mu$.

The bound-state energies of our theory will be found as the poles of the electron-nucleus to electron-nucleus two-particle Green's function. These poles are most conveniently obtained by working with a three-dimensional "quasipotential" formulation, to which we now turn.

The truncated Green's function of our theory, with momentum assignments shown in Fig. 1, satisfies the Bethe-Salpeter equation

$$\bar{G}_T(E;q,p) = \bar{K}(E;q,p) + \int \frac{d^4k}{(2\pi)^4}\bar{K}(E;q,k) \times \bar{S}(E;k)\bar{G}_T(E;k,p). \tag{A6}$$

In general, $\bar{K}$ represents all two-particle irreducible kernels. We consider here only those contributions to $\bar{K}$ that connect the electron and nucleus directly, ignoring contributions from photons that begin and end on the same charged particle. In this same approximation we ignore self-energy corrections in the electron-nucleus two-particle propagator, and have simply

$$\bar{S}(E;p) = \frac{i}{\gamma(P_e + p) - m + i\epsilon}\frac{i}{-p_0 - \frac{\vec{p}^2}{2M} + i\epsilon}. \tag{A7}$$

Our three-dimensional formalism is obtained by constructing a "reference" two-particle propagator

$$\tilde{S}(E;p) = \frac{i}{\gamma(P_e + p) - m + i\epsilon} 2\pi\delta\left(p_0 + \frac{\vec{p}^2}{2M}\right), \tag{A8}$$

which effectively forces the nucleus onto its mass shell (at least in the nonrelativisitic limit). We write a new equation for the truncated Green's function

$$\bar{G}_T(E;q,p) = \tilde{K}(E;q,p) + \int \frac{d^4k}{(2\pi)^4}\tilde{K}(E;q,k)\tilde{S}(E;k)\bar{G}_T(E;k,p), \tag{A9}$$

with a new kernel $\tilde{K}$ that is related to but not identical to $\bar{K}$. The delta function in $\tilde{S}$ puts the nucleus on shell inside of the momentum integration in Eq. (A9), and we do the same for external momenta by defining

$$G_T(E;\vec{q},\vec{p}) = i\gamma^0\bar{G}_T(E;\bar{q},\bar{p}),$$

$$V(E;\vec{q},\vec{p}) = i\gamma^0\tilde{K}(E;\bar{q},\bar{p}),$$

$$S(E;\vec{p}) = [\gamma(P_e + \bar{p}) - m + i\epsilon]^{-1}\gamma^0, \tag{A10}$$

where $\bar{q} = (-\vec{q}^2/2M, \vec{q})$ and $\bar{p} = (-\vec{p}^2/2M, \vec{p})$. The idea is to start with the original $\bar{G}_T$, a function of the four momenta, and put the nucleus on shell to arrive at the new G_T, a function of the three momenta. The factors of i and γ^0 move us from relativistic field theory conventions to conventions convenient for a nonrelativistic interpretation. The resulting three-dimensional equation is

$$G_T(E;\vec{q},\vec{p}) = V(E;\vec{q},\vec{p}) + \int \frac{d^3k}{(2\pi)^3}V(E;\vec{q},\vec{k})S(E;\vec{k})G_T(E;\vec{k},\vec{p}). \tag{A11}$$

In the following we will often suppress three-dimensional integration and write this as

$$G_T = V + VSG_T. \tag{A12}$$

The three-dimensional kernel V is often called the "quasipotential."

A homogeneous bound-state equation can be obtained from Eq. (A12) by first forming the nontruncated Green's function

$$G = S + SG_TS, \tag{A13}$$

which satisfies

$$G = S + SVG, \tag{A14}$$

and examining its pole structure. The energy poles of G are the same as those of G_T—that is, they are at the energies of the bound states for the problem. We define wave functions according to

$$G(E;\vec{p},\vec{q}) \to \frac{\psi(\vec{p})\psi^\dagger(\vec{q})}{E - \mathcal{E}}, \tag{A15}$$

as $E \to \mathcal{E}$ for bound-state energy $\mathcal{E}$. Then ψ satisfies a Dirac-type equation

$$\psi = SV\psi, \tag{A16}$$

or explicitly

$$(\mathcal{E} - \vec{p}^2/2M - \vec{\alpha}\cdot\vec{p} - \beta m)\psi(\vec{p}) = \int \frac{d^3q}{(2\pi)^3}V(\mathcal{E};\vec{p},\vec{q})\psi(\vec{q}). \tag{A17}$$

In the usual Bethe-Salpeter formalism, we would attempt to choose a reference propagator and kernel so that a reference Bethe-Salpeter equation could be exactly solved, and build a perturbation scheme about that exact solution that relies on the smallness of $Z\alpha$. As mentioned above, our approach here will be different. We will use m/M as our small parameter, with the expectation that the Dirac-Coulomb problem will provide the lowest-order point of reference. Coulomb photons must be dealt with to all orders in $Z\alpha$: it is clear from the NRQED interactions of Eq. (A3) that only transverse photons are suppressed by powers of $1/M$. Due to the need to account for all orders of Coulomb interactions, it is useful to eschew dealing with the Bethe-Salpeter kernel $\bar{K}$ and its complicated two-particle irreducible nature, and instead work with the full truncated Green's function G_T. Indeed, from Eq. (A12) we find that the quasipotential V is related to G_T according to

$$V = G_T(1 + SG_T)^{-1} = (1 + G_T S)^{-1} G_T. \tag{A18}$$

The lowest-order quasipotential is

$$V_0 = G_{T0}(1 + S_0 G_{T0})^{-1}, \tag{A19}$$

where S_0 and G_{T0} are just S and G_T in the large-M limit. This lowest-order potential will be obtained in the following subsection by working out G_{T0} explicitly. Moreover, the first-order correction to V due to $1/M$ dependence of G_T and S is given by

$$\begin{aligned}\Delta V &= \Delta G_T(1 + S_0 G_{T0})^{-1} - G_{T0}(1 + S_0 G_{T0})^{-1}(\Delta S G_{T0} + S_0 \Delta G_T) \\ &\quad \times (1 + S_0 G_{T0})^{-1} \\ &= (1 - V_0 S_0)\Delta G_T(1 - S_0 V_0) - V_0 \Delta S V_0,\end{aligned} \tag{A20}$$

where we have used $(1+G_T S)^{-1}=1-VS$ and $(1+SG_T)^{-1}=1-SV$.

Application of first-order perturbation theory to the quasipotential equation (A17) yields

$$\Delta \mathcal{E} = \left\langle \Delta V + \frac{\vec{p}^2}{2M} \right\rangle \tag{A21}$$

as the first-order energy correction. Here $\langle X\rangle = \psi_0^\dagger X \psi_0$, where ψ_0 satisfies the lowest-order quasipotential equation $\psi_0 = S_0 V_0 \psi_0$ with energy $\mathcal{E}_0$. The second term in ΔV of Eq. (A20) involves

$$\Delta S = S_0 \left(\frac{\vec{p}^2}{2M} \right) S_0, \tag{A22}$$

which cancels the $\vec{p}^2/2M$ term in Eq. (A21) leaving

$$\Delta \mathcal{E} = \langle (1 - V_0 S_0)\Delta G_T(1 - S_0 V_0) \rangle \tag{A23}$$

as the recoil correction to the energy at order $1/M$. The role of the $(1-V_0S_0)=G_0^{-1}S_0$ and $(1-S_0V_0)=S_0G_0^{-1}$ factors surrounding ΔG_T will soon become apparent: they serve to remove factors of the lowest-order Green's function that surround much of the actual perturbation present in ΔG_T. We make note now of one subtlety: the $(1-V_0S_0)$ and $(1-S_0V_0)$ factors in fact vanish when acting on lowest-order wave functions. We imagine evaluating $(1-V_0S_0)\Delta G_T(1-S_0V_0)$ at an energy slightly different from the bound state energy $\mathcal{E}_0$, affecting the cancellation discussed above, and only then setting the energy to $\mathcal{E}_0$.

2. Lowest-order kernel

In this section we show that the lowest-order kernel is just the usual Coulomb interaction, and the lowest-order quasipotential equation is the standard Dirac-Coulomb equation. The discussion here reprises the well-known result that the sum of all ladders and crossed ladders in the large mass limit gives the Dirac-Coulomb equation. Our purpose for reproducing this argument in some detail is to introduce notation that will be used in following sections to obtain the $1/M$ corrections.

We begin with an example. Figure 6 shows one of the six contributions to G_{T0} involving three photons. [The full set is shown in Fig. 3: this is graph 3(c).] The nucleus momenta for this graph are $v_1=-p_i+a_3$ and $v_2=-p_i+a_3+a_1$. Application of the Feynman rules (in the large-M limit) yields for this graph

$$\begin{aligned}G_{T0}^{(3c)}(E;\vec{p}_f,\vec{p}_i) &= i\gamma^0 \int \frac{d^4q_1}{(2\pi)^4}\frac{d^4q_2}{(2\pi)^4}(-ie\gamma^0)[iS_0(E+q_2^0;\vec{q}_2)\gamma^0](-ie\gamma^0)[iS_0(E+q_1^0;\vec{q}_1)\gamma^0](-ie\gamma^0) \\ &\quad \times \frac{i}{\vec{a}_1^2}\frac{i}{\vec{a}_2^2}\frac{i}{\vec{a}_3^2}(iZe)\frac{i}{a_3^0 + a_1^0 + i\epsilon}(iZe)\frac{i}{a_3^0 + i\epsilon}(iZe) \\ &= \int \frac{d^3q_1}{(2\pi)^3}\frac{d^3q_2}{(2\pi)^3} dq_1^0 dq_2^0 V_C(\vec{p}_f - \vec{q}_2) S_0(E + q_2^0;\vec{q}_2) V_C(\vec{q}_2 - \vec{q}_1) S_0(E + q_1^0;\vec{q}_1) V_C(\vec{q}_1 - \vec{p}_i)\delta_+(a_1^0 + a_3^0)\delta_+(a_3^0),\end{aligned} \tag{A24}$$

where

$$V_C(\vec{k}) = \frac{-4\pi Z\alpha}{\vec{k}^2}, \tag{A25}$$

$$S_0(E;\vec{p}) = \frac{1}{E - H}, \tag{A26}$$

$$H = \vec{\alpha}\cdot\vec{p} + \beta m(1 - i\epsilon), \tag{A27}$$

$$\delta_+(x) = \frac{i}{2\pi}\frac{1}{x + i\epsilon}. \tag{A28}$$

Now there are a total of six three-photon diagrams, and the only difference between one and another is in the nucleus propagator factors (that is, the δ_+s). One can show that

$$\sum_{S_3} \delta_+(a_i^0 + a_j^0)\delta_+(a_j^0) = \delta(a_1^0)\delta(a_2^0), \tag{A29}$$

where the sum is over the permutations S_3 of the three index values. (This is an instance of an identity that holds for any

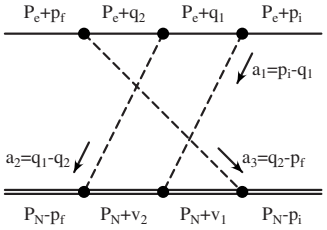

FIG. 6. One of the six contributions to the truncated Green's function G_{T0} involving three photons.

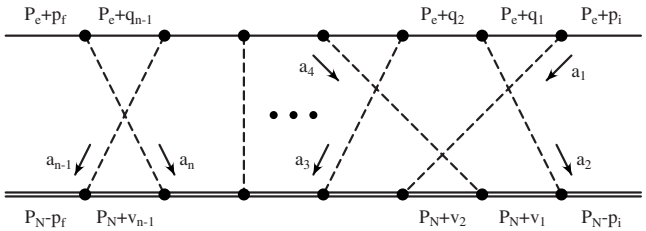

FIG. 7. An n-photon contribution to the truncated Green's function.

n, as we will soon see.) We use the delta functions to do the q_i^0 integrals, and find for the full three-photon contribution

$$G_{T0}^{(3)}(E;\vec{p}_f,\vec{p}_i) = \int \frac{d^3q_1}{(2\pi)^3}\frac{d^3q_2}{(2\pi)^3} V_C(\vec{p}_f - \vec{q}_2) S_0(E;\vec{q}_2) \times V_C(\vec{q}_2 - \vec{q}_1) S_0(E;\vec{q}_1) V_C(\vec{q}_1 - \vec{p}_i), \tag{A30}$$

or, with understood integrations,

$$G_{T0}^{(3)} = V_C S_0 V_C S_0 V_C. \tag{A31}$$

An n-photon pure-Coulomb diagram is represented in Fig. 7. By analogy with Eq. (A24) above, the Feynman rules for this diagram lead to the expression

$$\begin{aligned} G_{T0}^{(na)}(E;\vec{p}_f,\vec{p}_i) = \int & \frac{d^3q_1}{(2\pi)^3}\cdots\frac{d^3q_{n-1}}{(2\pi)^3} dq_1^0\cdots dq_{n-1}^0 \\ & \times V_C(\vec{p}_f - \vec{q}_{n-1}) S_0(E + q_{n-1}^0;\vec{q}_{n-1}) \\ & \times V_C(\vec{q}_{n-1} - \vec{q}_{n-2})\cdots \\ & \times V_C(\vec{q}_2 - \vec{q}_1) S_0(E + q_1^0;\vec{q}_1) \\ & \times V_C(\vec{q}_1 - \vec{p}_i)\delta_+(a_n^0 + \cdots + a_1^0 + a_4^0 \\ & + a_2^0)\cdots\delta_+(a_4^0 + a_2^0)\delta_+(a_2^0). \end{aligned} \tag{A32}$$

We have arranged our choice of momenta so that the electron line and photon propagators are the same for all $n!$ diagrams of this order. One can see that $a_1 = p_i - q_1, \ldots, a_i = q_{i-1} - q_i, \ldots, a_n = q_{n-1} - p_f$. Individual diagrams at this order are specified by a particular permutation σ of the indices $1,2,\ldots,n$. We choose to label the photons 1 to n from right (initial) to left (final) along the electron line. The permutation σ is defined so that photon $\sigma(i)$ connects to position i on the nucleus line with positions labeled 1 to n from right to left along the nucleus line. [In the diagram shown: $\sigma(1) = 2, \sigma(2) = 4, \ldots, \sigma(n) = n-1$.] Then one has $v_1 = a_{\sigma(1)} - p_i$, $v_2 = a_{\sigma(2)} + a_{\sigma(1)} - p_i, \ldots, v_{n-1} = a_{\sigma(n-1)} + \cdots + a_{\sigma(1)} - p_i$. The full n-photon contribution to G_{T0} is thus

$$\begin{aligned} G_{T0}^{(n)}(E;\vec{p}_f,\vec{p}_i) = \int & \frac{d^3q_1}{(2\pi)^3}\cdots\frac{d^3q_{n-1}}{(2\pi)^3} dq_1^0\cdots dq_{n-1}^0 V_C(\vec{p}_f \\ & - \vec{q}_{n-1}) S_0(E + q_{n-1}^0;\vec{q}_{n-1}) V_C(\vec{q}_{n-1} \\ & - \vec{q}_{n-2})\cdots V_C(\vec{q}_2 - \vec{q}_1) S_0(E + q_1^0;\vec{q}_1) V_C(\vec{q}_1 \\ & - \vec{p}_i) \sum_{\sigma\in S_n} \delta_+(a_{\sigma(n-1)}^0 + \cdots + a_{\sigma(1)}^0)\cdots\delta_+(a_{\sigma(2)}^0 \\ & + a_{\sigma(1)}^0)\delta_+(a_{\sigma(1)}^0). \end{aligned} \tag{A33}$$

It is useful at this point to examine carefully the properties of the δ_+ functions.

We define functions δ_+ and δ_- according to

$$\delta_\pm(x) \equiv \frac{i}{2\pi}\frac{1}{\pm x + i\epsilon}, \tag{A34}$$

where ϵ is a positive infinitesimal. Then $\delta_\pm$ can be expanded in terms of the principal part as

$$\delta_\pm(x) = \frac{\pm i}{2\pi}\mathrm{P}\left(\frac{1}{x}\right) + \frac{1}{2}\delta(x). \tag{A35}$$

Immediate consequences are

$$\delta_+(-x) = \delta_-(x), \tag{A36}$$

$$\delta_+(x) + \delta_-(x) = \delta(x). \tag{A37}$$

An addition rule states that

$$\delta_\pm(x) + \delta_\pm(y) = \frac{\delta_\pm(x)\delta_\pm(y)}{\delta_\pm(x+y)}, \tag{A38}$$

or in general

$$\frac{1}{\delta_\pm(x)} + \frac{1}{\delta_\pm(y)} + \cdots = \frac{1}{\delta_\pm(x + y + \cdots)}. \tag{A39}$$

We will now deal with the nucleus denominators. The nucleus factor from a diagram like that shown in Fig. 7 has the form

$$\begin{aligned} N(a_{\sigma(n)}^0,\cdots,a_{\sigma(1)}^0) \equiv & \delta_+(a_{\sigma(n-1)}^0 + \cdots a_{\sigma(1)}^0)\cdots\delta_+(a_{\sigma(2)}^0 \\ & + a_{\sigma(1)}^0)\delta_+(a_{\sigma(1)}^0). \end{aligned} \tag{A40}$$

We find it useful to define

$$\begin{aligned} \{x_n,\ldots,x_1\}_\pm \equiv & \sum_{\sigma\in S_n} \delta_\pm(x_{\sigma(n)} + \cdots x_{\sigma(1)})\cdots\delta_\pm(x_{\sigma(2)} \\ & + x_{\sigma(1)})\delta_\pm(x_{\sigma(1)}), \end{aligned} \tag{A41}$$

so that the sum of all $n!$ nth order graphs has the nucleus factor

$$N_n \equiv \sum_{\sigma\in S_n} N(a_{\sigma(n)}^0,\ldots,a_{\sigma(1)}^0) = \frac{\{a_n^0,\ldots,a_1^0\}_+}{\delta_+(a_n^0 + \cdots + a_1^0)}. \tag{A42}$$

A crucial fact about $\{x_n,\ldots,x_1\}_\pm$ is that

$$\{x_n,\ldots,x_1\}_\pm = \delta_\pm(x_n)\cdots\delta_\pm(x_1). \tag{A43}$$

We demonstrate this by induction. For $n=1$ we immediately have $\{x_1\}_\pm=\delta_\pm(x_1)$. The assertion for $n=2$ also follows simply from Eq. (A38). Now we assume that Eq. (A43) is true for $n-1$ elements. It follows that

$$\begin{aligned}\{x_n,\ldots,x_1\}_\pm &= \delta_\pm(x_n+\cdots+x_1)\sum_{\sigma\in S_n}\delta_\pm(x_{\sigma(n-1)}+\cdots \\ &\quad +x_{\sigma(1)})\cdots\delta_\pm(x_{\sigma(1)}) \\ &= \delta_\pm(x_n+\cdots+x_1)\sum_{j=1}^{n}\{x_n,\ldots,\underline{x_j},\ldots,x_1\}_\pm \\ &= \delta_\pm(x_n+\cdots+x_1)\sum_{j=1}^{n}\delta_\pm(x_n)\cdots\underline{\delta_\pm(x_j)}\cdots\delta_\pm(x_1) \\ &= \delta_\pm(x_n+\cdots+x_1)\left(\sum_{j=1}^{n}\frac{1}{\delta_\pm(x_j)}\right) \\ &\quad \times\delta_\pm(x_n)\cdots\delta_\pm(x_1)=\delta_\pm(x_n)\cdots\delta_\pm(x_1),\end{aligned} \tag{A44}$$

where the underlines denote terms that are missing. This completes the proof of Eq. (A43). So the nucleus factor of Eq. (A42) is

$$N_n = \frac{\delta_+(a_n^0)\cdots\delta_+(a_1^0)}{\delta_+(a_n^0+\cdots+a_1^0)}. \tag{A45}$$

The further evaluation of N_n requires some care when any of the a_i^0 vanish. Perhaps the most direct way to simplify N_n was given by Brodsky [24] using a method that he attributed to unpublished notes of Don Yennie. One needs to use the fact that $a_1^0+\cdots+a_n^0=0$ (which holds in the large M limit). Then, by using the addition rule (A38) $n-1$ times, one finds

$$\begin{aligned}N_n &= [\delta_+(a_n^0)+\delta_+(a_{n-1}^0+\cdots+a_1^0)]\frac{\delta_+(a_{n-1}^0)\cdots\delta_+(a_1^0)}{\delta_+(a_{n-1}^0+\cdots+a_1^0)} \\ &= \delta(a_{n-1}^0+\cdots+a_1^0)\frac{\delta_+(a_{n-1}^0)\cdots\delta_+(a_1^0)}{\delta_+(a_{n-1}^0+\cdots+a_1^0)} \\ &= \cdots \\ &= \delta(a_{n-1}^0+\cdots+a_1^0)\cdots\delta(a_2^0+a_1^0)\delta(a_1^0) \\ &= \delta(a_{n-1}^0)\cdots\delta(a_2^0)\delta(a_1^0).\end{aligned} \tag{A46}$$

This is the result, the generalization of Eq. (A29), that we need in order to complete the evaluation of G_{T0}. However, before we return to G_{T0}, we pause to consider an alternate approach to the evaluation of N_n that will help us in dealing with the kinds of nucleus expressions that occur in the $O(1/M)$ corrections. We consider first a particular nucleus factor of the form (A40). We can always write this factor with no explicit a_n^0 through use of $a_n^0+\cdots+a_1^0=0$. For example, with $n=4$ we can write

$$\begin{aligned}N(a_1^0,a_2^0,a_4^0,a_3^0) &= \delta_+(a_2^0+a_4^0+a_3^0)\delta_+(a_4^0+a_3^0)\delta_+(a_3^0) \\ &= \delta_-(a_1^0)\delta_-(a_1^0+a_2^0)\delta_+(a_3^0).\end{aligned} \tag{A47}$$

Propagator factors to the left of the vertex with the photon carrying momentum a_4 are written in terms of δ_- instead of δ_+, and reference to a_4^0 is eliminated. The general construction is

$$N_n = \sum_{\text{partitions }X,Y}\{X\}_-\{Y\}_+, \tag{A48}$$

where X and Y are partitions of $\{a_{n-1}^0,\ldots,a_1^0\}$. (That is, X and Y are disjoint, possibly empty, subsets of $\{a_{n-1}^0,\ldots,a_1^0\}$ such that every element of $\{a_{n-1}^0,\ldots,a_1^0\}$ is in one or the other of them.) This can be reexpressed by use of the identity (A43) as

$$N_n = \sum_{\text{partitions }X,Y}\prod_{j,a_j^0\in X}\delta_-(a_j^0)\prod_{k,a_k^0\in Y}\delta_+(a_k^0). \tag{A49}$$

Every term in this sum is a product of δ_- or δ_+ factors, one for each a_i^0 $(1\le i\le n-1)$. The sum over partitions brings in all possible combinations of δ_- and δ_+ factors. In other words, we again have

$$N_n = \prod_{i=1}^{n-1}[\delta_+(a_i^0)+\delta_-(a_i^0)] = \delta(a_{n-1}^0)\cdots\delta(a_1^0). \tag{A50}$$

Returning to our evaluation of $G_{T0}^{(n)}$, we can use Eq. (A50) to do the q_i^0 integrals in Eq. (A33). We find that

$$\begin{aligned}G_{T0}^{(n)}(E;\vec{p}_f,\vec{p}_i) &= \int\frac{d^3q_1}{(2\pi)^3}\cdots\frac{d^3q_{n-1}}{(2\pi)^3}V_C(\vec{p}_f-\vec{q}_{n-1})S_0(E;\vec{q}_{n-1}) \\ &\quad\times V_C(\vec{q}_{n-1}-\vec{q}_{n-2})\cdots V_C(\vec{q}_2-\vec{q}_1) \\ &\quad\times S_0(E;\vec{q}_1)V_C(\vec{q}_1-\vec{p}_i),\end{aligned} \tag{A51}$$

or

$$G_{T0}^{(n)} = V_C(S_0V_C)^{n-1}. \tag{A52}$$

The full truncated Green's function is thus

$$G_{T0} = \sum_{n=1}^{\infty}V_C(S_0V_C)^{n-1} = V_C(1-S_0V_C)^{-1}, \tag{A53}$$

which is exactly the truncated Dirac-Coulomb Green's function. It is no surprise then that use of Eq. (A19) leads to

$$\begin{aligned}V_0 &= G_{T0}(1+S_0G_{T0})^{-1} \\ &= V_C(1-S_0V_C)^{-1}\{1+S_0V_C(1-S_0V_C)^{-1}\}^{-1}=V_C.\end{aligned} \tag{A54}$$

In the large-M limit, our quasipotential is the usual Coulomb potential, and our lowest-order wave functions ψ_0 are the standard Dirac-Coulomb wave functions.

3. Pure-Coulomb contribution

Our goal in this section is to work out the recoil correction at $O(1/M)$ due to graphs containing only Coulomb photons. The Coulomb-nucleus vertex factor is simply iZe, so graphs with an arbitrarily large number of Coulomb photons must all be considered. The propagator for a nucleus carrying momentum P_N+v_k is $2\pi\delta_+(v_k^0-\vec{v}_k^2/2M)$. There are $O(1/M)$

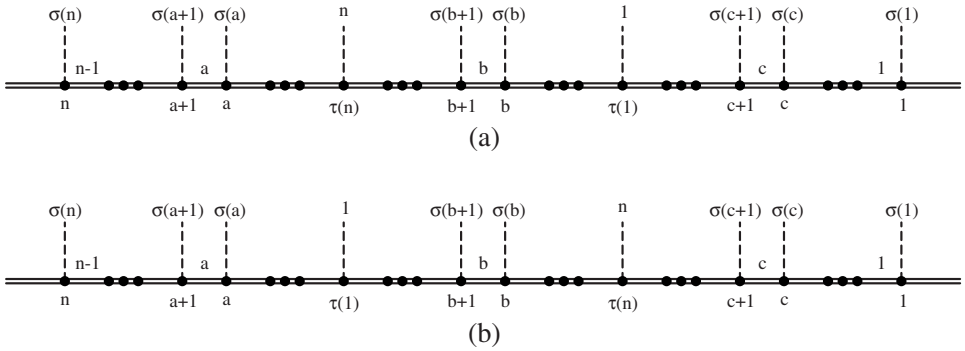

FIG. 8. Representation of the nucleus line in $\Delta G_T^{C(n)}$. The numbers below the line label position on that line, from 1 on the right to n on the left. Several incoming Coulomb photons are shown. The numbers above the photons label the photons, and correspond to position on the electron line (which isn't shown here). The photon entering at position j is labeled $\sigma(j)$, and photon k attaches to position $\tau(k)$, where $\tau=\sigma^{-1}$. Part (a) represents the situation where the nth photon enters the nucleus line to the left of the first one, and (b) shows the opposite ordering of these two. Photons $\sigma(a)$, $\sigma(b)$, and $\sigma(c)$ represent photons entering to the left of photons 1 and n, between them, or to the right of them. The numbers just above the nucleus line label the line segments, numbered right to left from 1 to $n-1$.

corrections in this propagator coming from both the explicit $1/M$ in the $\vec{v}_k^2/2M$ term and also $\vec{p}_i^2/2M$ or $\vec{p}_f^2/2M$ parts from v_k^0 for some of the propagators. Now if $v_k^0=\vec{v}_k^0+\vec{v}_k^0/2M$ is the sum of an M-independent part and a $1/M$ correction, then the kth nucleus propagation factor has a $1/M$ correction equal to

$$\Delta\,\delta_+(v_k^0-\vec{v}_k^2/2M)=\delta_+(\vec{v}_k^0)\left\{\frac{-i\pi}{M}(\vec{v}_k^2-\vec{v}_k^0)\right\}\delta_+(\vec{v}_k^0). \tag{A55}$$

With our momentum routing the only M dependence in the pure-Coulomb truncated Green's function is in the nucleus line, and $G_T^{C(n)}$ has just the form of Eq. (A33) except that the nucleus line factor is instead

$$\sum_{\sigma\in S_n}\delta_+\left(v_{\sigma(n-1)}^0-\frac{\vec{v}_{\sigma(n-1)}^2}{2M}\right)\cdots\delta_+\left(v_{\sigma(1)}^0-\frac{\vec{v}_{\sigma(1)}^2}{2M}\right). \tag{A56}$$

It follows that the first-order perturbation has the form

$$\Delta G_T^{C(n)}(E;\vec{p}_f,\vec{p}_i)=\frac{-i\pi}{M}\int\frac{d^3q_1}{(2\pi)^3}\cdots\frac{d^3q_{n-1}}{(2\pi)^3}dq_1^0\cdots dq_{n-1}^0V_C(\vec{p}_f-\vec{q}_{n-1})S_0(E+q_{n-1}^0;\vec{q}_{n-1})\times V_C(\vec{q}_{n-1}-\vec{q}_{n-2})\cdots V_C(\vec{q}_2-\vec{q}_1)S_0(E+q_1^0;\vec{q}_1)V_C(\vec{q}_1-\vec{p}_i)\times\sum_{\sigma\in S_n}\left\{\sum_{k=1}^{n-1}(\vec{v}_k^2-\vec{v}_k^0)\delta_+(\vec{v}_k^0)\right\}\delta_+(\vec{v}_{n-1}^0)\cdots\delta_+(\vec{v}_1^0), \tag{A57}$$

where

$$v_k=\sum_{r=1}^{k}a_{\sigma(r)}-p_i=-\sum_{s=k+1}^{n}a_{\sigma(s)}-p_f. \tag{A58}$$

The nucleus factor in $\Delta G_T^{C(n)}$ is a quadratic function of the momenta $\vec{p}_i$, $\vec{p}_f$, $\vec{a}_k$ $(1\le k\le n)$. As can be seen from Eq. (A58), the nucleus line momentum vector can be written in two equivalent forms, and consequently, we have some freedom to choose how we represent the nucleus factor in $\Delta G_T^{C(n)}$. We choose to write it as a linear combination of $\vec{p}_i^2$, $\vec{p}_f^2$, $\vec{a}_k\cdot\vec{p}_i$, and $\vec{a}_k\cdot\vec{p}_f(1\le k\le n-1)$, and $\vec{a}_j\cdot\vec{a}_k$ $(1\le j,k\le n,\ j\ne k)$. This form of the nucleus factor proves convenient for further simplification. In order to avoid factors $\vec{a}_n\cdot\vec{p}_i$ and $\vec{a}_n\cdot\vec{p}_f$ in our expression for the nucleus factor it is important to know the position of each nucleus propagator relative to photon n so that the appropriate form of (A58) may be employed. Also, whether or not there are $\vec{p}_f^2$ or $\vec{p}_i^2$ factors in $\vec{v}^0$depends on the location of the nucleus propagator relative to both photons n and 1: there is a $\vec{p}_f^2$ when the propagator is to the left of photon n, and a $\vec{p}_i^2$ when the propagator is to the right of photon 1. We will examine the various situations in more detail. Figure 8 shows the nucleus line with various attached photons for the situations where (a) photon n lies to the left of photon 1, and (b) otherwise. In case (a), the $\vec{v}^2-\vec{v}^0$ factors for a nucleus propagator to the left of photon n,

between photons n and 1, and to the right of photon 1, take the forms

$$\vec{v}_a^2 - \vec{v}_a^0 = \vec{p}_f^2 + \sum_{s=a+1}^{n} \vec{a}_{\sigma(s)} \cdot (\vec{p}_i + \vec{p}_f) - \sum_{r=1}^{a} \vec{a}_{\sigma(r)} \cdot \sum_{s=a+1}^{n} \vec{a}_{\sigma(s)} - \vec{p}_f^2,$$

$$\vec{v}_b^2 - \vec{v}_b^0 = \vec{p}_i^2 - \sum_{r=1}^{b} \vec{a}_{\sigma(r)} \cdot (\vec{p}_i + \vec{p}_f) - \sum_{r=1}^{b} \vec{a}_{\sigma(r)} \cdot \sum_{s=b+1}^{n} \vec{a}_{\sigma(s)},$$

$$\vec{v}_c^2 - \vec{v}_c^0 = \vec{p}_i^2 - \sum_{r=1}^{c} \vec{a}_{\sigma(r)} \cdot (\vec{p}_i + \vec{p}_f) - \sum_{r=1}^{c} \vec{a}_{\sigma(r)} \cdot \sum_{s=c+1}^{n} \vec{a}_{\sigma(s)} - \vec{p}_i^2. \tag{A59}$$

The forms for case (b) are similar.

$$\vec{v}_a^2 - \vec{v}_a^0 = \vec{p}_f^2 + \sum_{s=a+1}^{n} \vec{a}_{\sigma(s)} \cdot (\vec{p}_i + \vec{p}_f) - \sum_{r=1}^{a} \vec{a}_{\sigma(r)} \cdot \sum_{s=a+1}^{n} \vec{a}_{\sigma(s)} - \vec{p}_f^2,$$

$$\vec{v}_b^2 - \vec{v}_b^0 = \vec{p}_f^2 + \sum_{s=b+1}^{n} \vec{a}_{\sigma(s)} \cdot (\vec{p}_i + \vec{p}_f) - \sum_{r=1}^{b} \vec{a}_{\sigma(r)} \cdot \sum_{s=b+1}^{n} \vec{a}_{\sigma(s)} - \vec{p}_f^2 - \vec{p}_i^2,$$

$$\vec{v}_c^2 - \vec{v}_c^0 = \vec{p}_i^2 - \sum_{r=1}^{c} \vec{a}_{\sigma(r)} \cdot (\vec{p}_i + \vec{p}_f) - \sum_{r=1}^{c} \vec{a}_{\sigma(r)} \cdot \sum_{s=c+1}^{n} \vec{a}_{\sigma(s)} - \vec{p}_i^2. \tag{A60}$$

In each situation the term $\vec{a}_n \cdot (\vec{p}_i + \vec{p}_f)$ has been avoided by an appropriate choice in Eq. (A58). It is clear that the $\vec{p}_f^2$ always cancels, and will not contribute to the final result. Also, $\vec{p}_i^2$ only appears in propagators lying between photons n and 1, with a plus sign when photon n is to the left of photon 1, and a minus sign when photon n is to the right of photon 1. The term $-\vec{a}_1 \cdot (\vec{p}_i + \vec{p}_f)$ appears under precisely the same conditions. The common coefficient of $\vec{p}_i^2$ and $-\vec{a}_1 \cdot (\vec{p}_i + \vec{p}_f)$ in the nucleus line factor is thus

$$\sum_{\sigma \in S_n} \left\{ \sum_{b=1}^{n-1} \chi(\sigma, b)\, \theta(\sigma, b)\, \delta_+(\tilde{v}_b^0) \right\} \delta_+(\tilde{v}_{n-1}^0) \cdots \delta_+(\tilde{v}_1^0), \tag{A61}$$

where $\chi(\sigma,b)$ is a sign: plus for photon n to the left of photon 1, minus otherwise, and $\theta(\sigma,b)$ is a θ function: one for propagator b between photon n and photon 1, zero otherwise. Considering the term with photon n to the left of photon 1, the contribution can be expressed as

$$\sum_{\text{partitions } X,Y} \{X\}_- \{Y\}_+ = \sum_{\text{partitions } X,Y} \prod_{j, \tilde{a}_j^0 \in X} \delta_-(\tilde{a}_j^0) \prod_{k, \tilde{a}_k^0 \in Y} \delta_+(\tilde{a}_k^0), \tag{A62}$$

where X and Y are partitions of $\{\tilde{a}_n^0, \ldots, \tilde{a}_1^0\}$ having $\tilde{a}_n^0 \in X$ and $\tilde{a}_1^0 \in Y$. (Note that all $\tilde{a}^0$s equal the corresponding a^0s except that $\tilde{a}_n^0 = q_{n-1}^0$ while $a_n^0 = q_{n-1}^0 + \vec{p}_f^2/2M$ and $\tilde{a}_1^0 = -q_1^0$ while $a_1^0 = -\vec{p}_i^2/2M - q_1^0$.) The sum over partitions brings in all possible combinations of δ_- and δ_+ factors except that $\tilde{a}_n^0$ only occurs inside of δ_-, and $\tilde{a}_1^0$ only occurs inside of δ_+. The partition sum then can be written as

$$\sum_{\text{partitions } X,Y} \{X\}_- \{Y\}_+ = \delta_-(\tilde{a}_n^0) \cdots \delta_+(\tilde{a}_1^0), \tag{A63}$$

where the dots indicate δ functions of the remaining $\tilde{a}^0$s. The term with photon n to the right of photon 1 is the same except that $\tilde{a}_n^0$ occurs inside of δ_+, $\tilde{a}_1^0$ occurs inside of δ_-, and there is a sign difference. The coefficient of $-\vec{a}_i \cdot (\vec{p}_i + \vec{p}_f)$ for any i is found in the same way: the only propagators that contribute lie between photons n and i, with signs as before. This coefficient is

$$\delta_-(\tilde{a}_n^0) \cdots \delta_+(\tilde{a}_i^0) \cdots \delta(\tilde{a}_1^0) - \delta_+(\tilde{a}_n^0) \cdots \delta_-(\tilde{a}_i^0) \cdots \delta(\tilde{a}_1^0), \tag{A64}$$

where the dots have the same meaning as in Eq. (A63). Finally, it is evident from Eqs. (A59) and (A60) that the contributions to the coefficient of $-\vec{a}_i \cdot \vec{a}_j$ come only from propagators lying between photons i and j, all with the same sign. The coefficient is thus

$$\delta(\tilde{a}_n^0) \cdots \delta_-(\tilde{a}_i^0) \cdots \delta_+(\tilde{a}_j^0) \cdots \delta(\tilde{a}_1^0) + \delta(\tilde{a}_n^0) \cdots \delta_+(\tilde{a}_i^0) \cdots \delta_-(\tilde{a}_j^0) \cdots \delta(\tilde{a}_1^0). \tag{A65}$$

In all, the perturbation $\Delta G_T^{C(n)}$ takes the form

$$\Delta G_T^{C(n)}(E;\vec{p}_f,\vec{p}_i) = \frac{-i\pi}{M} \int \frac{d^3q_1}{(2\pi)^3} \cdots \frac{d^3q_{n-1}}{(2\pi)^3} dq_1^0 \cdots dq_{n-1}^0 V_C(\vec{p}_f - \vec{q}_{n-1}) S_0(E + q_{n-1}^0; \vec{q}_{n-1}) V_C(\vec{q}_{n-1} - \vec{q}_{n-2}) \cdots V_C(\vec{q}_2 - \vec{q}_1) S_0(E + q_1^0; \vec{q}_1) V_C(\vec{q}_1 - \vec{p}_i) \left\{ \vec{p}_i^2 [\delta_-(\tilde{a}_n^0) \cdots \delta_+(\tilde{a}_1^0) - \delta_+(\tilde{a}_n^0) \cdots \delta_-(\tilde{a}_1^0)] - \sum_{i=1}^{n-1} \vec{a}_i \cdot (\vec{p}_i + \vec{p}_f) [\delta_-(\tilde{a}_n^0) \cdots \delta_+(\tilde{a}_i^0) \cdots \delta(\tilde{a}_1^0) - \delta_+(\tilde{a}_n^0) \cdots \delta_-(\tilde{a}_i^0) \cdots \delta(\tilde{a}_1^0)] - \sum_{i,j(i \neq j)=1}^{n} \vec{a}_i \cdot \vec{a}_j \delta(\tilde{a}_n^0) \cdots \delta_-(\tilde{a}_i^0) \cdots \delta_+(\tilde{a}_j^0) \cdots \delta(\tilde{a}_1^0) \right\}. \tag{A66}$$

Our next task is to perform or simplify the q^0 integrals using the delta functions, and at the same time to do the sum over n. The $\vec{p}_i^2$ term is easiest, so we begin there. We recall that $\tilde{a}_n^0 = q_{n-1}^0$, $\tilde{a}_{n-1}^0 = q_{n-2}^0 - q_{n-1}^0$, …, $\tilde{a}_2^0 = q_1^0 - q_2^0$, $\tilde{a}_1^0 = -q_1^0$, so most of the delta functions just set one q^0 equal to the next. This first contribution to $\Delta G_T^{C(n)}$ is

$$\Delta G_T^{C(n)1}(E;\vec{p}_f,\vec{p}_i) = \frac{-i\pi}{M}\int \frac{d^3q_1}{(2\pi)^3}\cdots\frac{d^3q_{n-1}}{(2\pi)^3}dq_1^0\cdots dq_{n-1}^0 V_C(\vec{p}_f-\vec{q}_{n-1})S_0(E+q_{n-1}^0;\vec{q}_{n-1})V_C(\vec{q}_{n-1}-\vec{q}_{n-2})\cdots V_C(\vec{q}_2-\vec{q}_1)S_0(E$$
$$+q_1^0;\vec{q}_1)V_C(\vec{q}_1-\vec{p}_i)\vec{p}_i^2\{[\delta_-^2(q_1^0)-\delta_+^2(q_1^0)]\delta(q_{n-1}^0-q_{n-2}^0)\cdots\delta(q_2^0-q_1^0)\}$$
$$=\frac{-i\pi}{M}\int d\omega[\delta_-^2(\omega)-\delta_+^2(\omega)]\int\frac{d^3q_1}{(2\pi)^3}\cdots\frac{d^3q_{n-1}}{(2\pi)^3}V_C(\vec{p}_f-\vec{q}_{n-1})S_0(E+\omega;\vec{q}_{n-1})\cdots V_C(\vec{q}_1-\vec{p}_i)\vec{p}_i^2, \tag{A67}$$

where we write ω for q_1^0. We pass to a notation in which the three-dimensional momentum integrals are implicit, and write

$$\Delta G_T^{C(n)1}(E) = \frac{-i\pi}{M}\int d\omega[\delta_-^2(\omega)-\delta_+^2(\omega)]V_C S_0(E+\omega)$$
$$\times[V_C S_0(E+\omega)]^{n-2}V_C\vec{p}^2. \tag{A68}$$

The sum over all values of n $(2\le n<\infty)$ gives

$$\Delta G_T^{C1}(E) = \frac{-i\pi}{M}\int d\omega[\delta_-^2(\omega)-\delta_+^2(\omega)]V_C G_C(E+\omega)V_C\vec{p}^2, \tag{A69}$$

where $G_C(E)$ is the Dirac-Coulomb Green's function

$$G_C(E) = S_0(E)[1-V_C S_0(E)]^{-1}. \tag{A70}$$

In order to perform the final energy integral, over ω, we use the spectral representation of the Dirac-Coulomb Green's function (which differs from the S_F of Eq. (1) by a factor of γ^0: $G_C=S_F\gamma^0$)

$$G_C(E) = \sum_m \frac{\psi_{0m}\psi_{0m}^\dagger}{E-\mathcal{E}_{0m}(1-i\epsilon)}, \tag{A71}$$

and do the ω integral by the residue theorem as follows:

$$\int d\omega[\delta_-^2(\omega)-\delta_+^2(\omega)]G_C(E+\omega) = \frac{-i}{2\pi}\int\frac{d\omega}{2\pi i}\left(\frac{1}{(\omega-i\epsilon)^2}-\frac{1}{(\omega+i\epsilon)^2}\right)\left\{\sum_{m,\mathcal{E}_{0m}>0}\frac{\psi_{0m}\psi_{0m}^\dagger}{E+\omega-\mathcal{E}_{0m}+i\epsilon}+\sum_{m,\mathcal{E}_{0m}<0}\frac{\psi_{0m}\psi_{0m}^\dagger}{E+\omega-\mathcal{E}_{0m}-i\epsilon}\right\}$$
$$=\frac{i}{2\pi}\left\{\sum_{m,\mathcal{E}_{0m}>0}\frac{\psi_{0m}\psi_{0m}^\dagger}{(E-\mathcal{E}_{0m}+i\epsilon)^2}+\sum_{m,\mathcal{E}_{0m}<0}\frac{\psi_{0m}\psi_{0m}^\dagger}{(E-\mathcal{E}_{0m}-i\epsilon)^2}\right\}$$
$$=\frac{i}{2\pi}G_C^2(E), \tag{A72}$$

where we have used the orthonormality of Dirac-Coulomb wave functions $\psi_{0n}^\dagger\psi_{0m}=\delta_{nm}$ in the reduction of G_C^2. We find that

$$\Delta G_T^{C1}(E) = \frac{1}{2M}V_C G_C^2(E)V_C\vec{p}^2. \tag{A73}$$

The second contribution to $\Delta G_T^{C(n)}$, coming from terms in Eq. (A66) involving $\vec{a}_i\cdot\vec{p}_i$, is

$$\Delta G_T^{C(n)2}(E;\vec{p}_f,\vec{p}_i) = \frac{-i\pi}{M}\int \frac{d^3q_1}{(2\pi)^3}\cdots\frac{d^3q_{n-1}}{(2\pi)^3}dq_1^0\cdots dq_{n-1}^0 V_C(\vec{p}_f-\vec{q}_{n-1})S_0(E+q_{n-1}^0;\vec{q}_{n-1})V_C(\vec{q}_{n-1}-\vec{q}_{n-2})\cdots V_C(\vec{q}_2-\vec{q}_1)S_0(E$$
$$+q_1^0;\vec{q}_1)V_C(\vec{q}_1-\vec{p}_i)\sum_{i=1}^{n-1}(-\vec{a}_i\cdot\vec{p}_i)\{\delta_-(\tilde{a}_n^0)\cdots\delta_+(\tilde{a}_i^0)\cdots\delta(\tilde{a}_1^0)-\delta_+(\tilde{a}_n^0)\cdots\delta_-(\tilde{a}_i^0)\cdots\delta(\tilde{a}_1^0)\}. \tag{A74}$$

Again, most of the energy integrals can be done immediately. Only one is left, that involving $q_i^0\equiv\omega$, and we find

$$\Delta G_T^{C(n)2}(E;\vec{p}_f,\vec{p}_i) = \frac{-i\pi}{M}\int d\omega[\delta_-^2(\omega)-\delta_+^2(\omega)]\sum_{i=1}^{n-1}\int\frac{d^3q_1}{(2\pi)^3}\cdots\frac{d^3q_{n-1}}{(2\pi)^3}V_C(\vec{p}_f-\vec{q}_{n-1})S_0(E+\omega;\vec{q}_{n-1})\cdots S_0(E+\omega;\vec{q}_i)\times[\vec{q}_i V_C(\vec{q}_i$$
$$-\vec{q}_{i-1})-V_C(\vec{q}_i-\vec{q}_{i-1})\vec{q}_{i-1}]\times S_0(E;\vec{q}_{i-1})\cdots S_0(E;\vec{q}_1)V_C(\vec{q}_1-\vec{p}_i)\cdot\vec{p}_i. \tag{A75}$$

With implicit three-dimensional integrations, this reads

$$\Delta G_T^{C(n)2}(E) = \frac{-i\pi}{M}\int d\omega[\delta_-^2(\omega) - \delta_+^2(\omega)] \times \sum_{i=1}^{n-1} [V_C S_0(E+\omega)]^{n-i}[\vec{p}, V_C][S_0(E)V_C]^{i-1}\cdot\vec{p}. \tag{A76}$$

A commutator structure arises because $\vec{a}_i$ is the difference between one momentum and the next. Now in the sum there are from 1 to $n-1$ factors of $V_C S_0(E+\omega)$ on the left of the commutator, and from 0 to $n-2$ factors of $S_0(E)V_C$ to the right. When we perform both the sum over i and the sum over n, the infinite sum builds up Green's-function-like factors in both positions. After performing the sums, this second correction term becomes

$$\Delta G_T^{C2}(E) = \frac{-i\pi}{M}\int d\omega[\delta_-^2(\omega) - \delta_+^2(\omega)]V_C G_C(E+\omega)[\vec{p}, V_C][1 - S_0(E)V_C]^{-1}\cdot\vec{p}. \tag{A77}$$

The final ω integral can be done as before, yielding

$$\Delta G_T^{C2}(E) = \frac{1}{2M}V_C G_C^2(E)[\vec{p}, V_C][1 - S_0(E)V_C]^{-1}\cdot\vec{p}. \tag{A78}$$

The calculation for the third contribution to $\Delta G_T^{C(n)}$, due to $\vec{a}_i\cdot\vec{p}_f$, is similar to the above, and gives

$$\Delta G_T^{C3}(E) = \frac{1}{2M}\vec{p}V_C G_C^2(E)\cdot[\vec{p}, V_C][1 - S_0(E)V_C]^{-1}. \tag{A79}$$

The fourth and final contribution to $\Delta G_T^{C(n)}$, the $\vec{a}_i\cdot\vec{a}_j$ part, is a bit different because here the $\delta_-^2(\omega)$ and $\delta_+^2(\omega)$ terms have the same sign. We set $\delta_-^2(\omega)+\delta_+^2(\omega) = [\delta_-^2(\omega) - \delta_+^2(\omega)] + 2\delta_+^2(\omega)$ and leave the ω integral undone in the $2\delta_+^2(\omega)$ term. The result for this contribution is

$$\Delta G_T^{C4}(E) = \frac{-1}{2M}[1 - V_C S_0(E)]^{-1}[\vec{p}, V_C]G_C^2(E)\cdot[\vec{p}, V_C][1 - S_0(E)V_C]^{-1} + \frac{2\pi i}{M}\int d\omega\delta_+^2(\omega)[1 - V_C S_0(E)]^{-1} \times [\vec{p}, V_C]G_C(E+\omega)\cdot[\vec{p}, V_C][1 - S_0(E)V_C]^{-1}. \tag{A80}$$

Our final task for the pure-Coulomb correction will be to combine and simplify the various contributions. The total pure-Coulomb correction, from Eqs. (A73) and (A78)–(A80), is

$$\Delta G_T^C = \frac{1}{2M}\{V_C G_C^2 V_C\vec{p}^2 + V_C G_C^2[\vec{p}, V_C](1 - S_0V_C)^{-1}\cdot\vec{p} + \vec{p}V_C G_C^2\cdot[\vec{p}, V_C](1 - S_0V_C)^{-1} - (1 - V_C S_0)^{-1} \times [\vec{p}, V_C]G_C^2\cdot[\vec{p}, V_C](1 - S_0V_C)^{-1}\} + \frac{2\pi i}{M}\int d\omega\delta_+^2(\omega) \times (1 - V_C S_0)^{-1}[\vec{p}, V_C]G_C(E+\omega)\cdot[\vec{p}, V_C](1 - S_0V_C)^{-1}. \tag{A81}$$

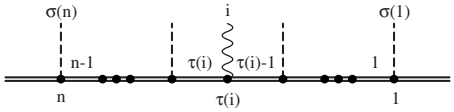

FIG. 9. A typical one-transverse-photon graph with n photons showing the nucleus line only. The numbers above the various photons label the photons according to their order on the electron line. The numbers below the nucleus line indicate the ordering of photons on that line, from 1 on the right to n on the left. The numbers just above the nucleus line label the nucleus propagators: the propagator labeled k carries momentum P_N+v_k.

Each of the integrated terms is quadratic in $G_C(E)$. The double pole at each lowest-order bound-state energy is removed by surrounding ΔG_T^C with $(1-V_C S_0)\cdots(1-S_0V_C)$ factors as in Eq. (A23). In fact, the integrated part reduces to a surprisingly simple form. After an algebraic reduction, one finds that

$$(1 - V_C S_0)\Delta G_T^C(1 - S_0V_C) = V_C S_0\frac{\vec{p}^2}{2M}S_0V_C + \frac{2\pi i}{M}\int d\omega\delta_+^2(\omega) \times [\vec{p}, V_C]G_C(E+\omega)\cdot[\vec{p}, V_C]. \tag{A82}$$

Finally, we arrive at the pure-Coulomb recoil correction

$$\Delta\mathcal{E}^C = \left\langle\frac{\vec{p}^2}{2M}\right\rangle + \frac{2\pi i}{M}\int d\omega\delta_+^2(\omega)\langle[\vec{p}, V_C] \times G_C(\mathcal{E}_0+\omega)\cdot[\vec{p}, V_C]\rangle. \tag{A83}$$

In this final step we set the energy E running through $(1-V_C S_0)\Delta G_T^C(1-S_0V_C)$ equal to the lowest-order bound-state energy $\mathcal{E}_0$, and made use of the Dirac-Coulomb equation $S_0V_C\psi_0 = \psi_0$.

4. One-transverse-photon contribution

We turn now to the evaluation of the one-transverse-photon contribution. A single transverse photon brings with it an explicit $1/M$ due to the Feynman rule of Eq. (A3), and so all other $1/M$ complications in the nucleus propagator and external momentum can be ignored. However, an arbitrary number of Coulomb photons can accompany the transverse photon. For a given total photon number n there are now $n\times n!$ possible graphs: the factor of n describes the multiplicity of locations for the transverse photon to attach to the electron line, and $n!$ is the number of possible ways for the n photons, ordered by their position on the electron line, to attach to the nucleus line. A typical one-transverse-photon graph is represented in Fig. 9. By analogy with the pure-Coulomb contribution to G_T given in Eq. (A33), the one-transverse-photon correction is

$$\Delta G_T^{T(n)}(E;\vec{p}_f,\vec{p}_i) = \sum_{i=1}^{n}\int\frac{d^3q_1}{(2\pi)^3}\cdots\frac{d^3q_{n-1}}{(2\pi)^3}dq_1^0\cdots dq_{n-1}^0 \times V_C(\vec{p}_f - \vec{q}_{n-1})S_0(E + q_{n-1}^0;\vec{q}_{n-1}) \times V_C(\vec{q}_{n-1} - \vec{q}_{n-2})\cdots$$

$$\times S_0(E+q_i^0;\vec{q}_i)D_b(q_i-q_{i-1})$$
$$\times S_0(E+q_{i-1}^0;\vec{q}_{i-1})\cdots S_0(E+q_1^0;\vec{q}_1)V_C(\vec{q}_1$$
$$-\vec{p}_i)\sum_{\sigma\in S_n}\left\{\frac{Q_i^b}{2M}\right\}\delta_+(v_{n-1}^0)\cdots\delta_+(v_1^0), \tag{A84}$$

where $Q_i^b=(v_{\tau(i)}+v_{\tau(i)-1})^b$, and

$$i\gamma^0(-ie\gamma^0)\frac{i}{\vec{q}^2}(iZe)=\frac{-4\pi Z\alpha}{\vec{q}^2}\equiv V_C(\vec{q}),$$

$$i\gamma^0(-ie\gamma^a)iD_{ab}(q)(iZe)=(-4\pi Z\alpha)\alpha^a D_{ab}(q)\equiv D_b(q). \tag{A85}$$

Now the two contributions to $\vec{Q}_i$ have clear graphical meanings: $\vec{v}_{\tau(i)-1}$ is $-\vec{p}_i$ plus the sum of all $\vec{a}$s that enter the electron line to the right of the transverse photon at position i, and $\vec{v}_{\tau(i)}$ is $-\vec{p}_f$ minus the sum of all $\vec{a}$s that enter the electron line to the left of the transverse photon at position i. When we choose to write $\vec{v}_{\tau(i)-1}$ and $\vec{v}_{\tau(i)}$ in this way, no term proportional to $\vec{a}_i$is present in $\vec{Q}_i$. In fact, we can write the nucleus line factor as

$$\sum_{\sigma\in S_n}\vec{Q}_i N(a_{\sigma(n)}^0,\ldots,a_{\sigma(1)}^0)=-A(\vec{p}_i+\vec{p}_f)+\sum_{k=1(k\neq i)}^{n}B_k\vec{a}_k \tag{A86}$$

for some coefficients A,B_k. Since the part of $\vec{Q}_i$ involving $\vec{p}_i$ and $\vec{p}_f$ is exactly $-(\vec{p}_i+\vec{p}_f)$ for all σ, the coefficient A is just

$$A=\sum_{\sigma\in S_n}N(a_{\sigma(n)}^0,\ldots,a_{\sigma(1)}^0)=N_n=\delta(a_{n-1}^0)\cdots\delta(a_1^0). \tag{A87}$$

Now the momentum $\vec{a}_k$ occurs in $\vec{Q}_i$ with a plus sign when photon k enters the nucleus line to the right of photon i, and with a minus sign when photon k enters to the left of photon i, so that

$$B_k=\sum_{\text{partitions }X,Y}\{X\}_-\{Y\}_+-\sum_{\text{partitions }X',Y'}\{X'\}_-\{Y'\}_+, \tag{A88}$$

where X, Y and X', Y' are partitions of $\{a_n^0,\ldots,\underline{a_i^0},\ldots a_1^0\}$ with $a_k^0\in Y$ and $a_k^0\in X'$. It follows that

$$B_k=\delta(a_n^0)\cdots\underline{\delta(a_k^0)}\cdots\underline{\delta(a_i^0)}\cdots\delta(a_1^0)(\delta_+(a_k^0)-\delta_-(a_k^0)), \tag{A89}$$

where again the underlines signify omitted terms. Now we are prepared to do the q^0 integrals in Eq. (A84). The first part, proportional to $\vec{p}_i+\vec{p}_f$, is

$$\Delta G_T^{T(n)1}(E;\vec{p}_f,\vec{p}_i)=\frac{-1}{2M}\sum_{i=1}^{n}\int\frac{d^3q_1}{(2\pi)^3}\cdots\frac{d^3q_{n-1}}{(2\pi)^3}V_C(\vec{p}_f-\vec{q}_{n-1})$$
$$\times S_0(E;\vec{q}_{n-1})\cdots S_0(E;\vec{q}_i)D_b(0;\vec{q}_i-\vec{q}_{i-1})$$
$$\times S_0(E;\vec{q}_{i-1})\cdots S_0(E;\vec{q}_1)V_C(\vec{q}_1-\vec{p}_i)$$
$$\times(p_i+p_f)^b, \tag{A90}$$

or briefly,

$$\Delta G_T^{T(n)1}(E)=\frac{-1}{2M}\sum_{i=1}^{n}\{(V_CS_0(E))^{n-i}D_b(0)(S_0(E)V_C)^{i-1}p^b$$
$$+p^b(V_CS_0(E))^{n-i}D_b(0)(S_0(E)V_C)^{i-1}\}. \tag{A91}$$

After performing the sum over n this becomes

$$\Delta G_T^{T1}(E)=\frac{-1}{2M}\{[1-V_CS_0(E)]^{-1}D_b(0)[1-S_0(E)V_C]^{-1}p^b$$
$$+p^b[1-V_CS_0(E)]^{-1}D_b(0)[1-S_0(E)V_C]^{-1}\}. \tag{A92}$$

The second one-transverse-photon contribution is a bit more complicated to evaluate. It is

$$\Delta G_T^{T(n)2}(E;\vec{p}_f,\vec{p}_i)=\frac{1}{2M}\sum_{i=1}^{n}\int\frac{d^3q_1}{(2\pi)^3}\cdots\frac{d^3q_{n-1}}{(2\pi)^3}dq_1^0\cdots dq_{n-1}^0$$
$$\times V_C(\vec{a}_n)S_0(E+q_{n-1}^0;\vec{q}_{n-1})\cdots$$
$$\times S_0(E+q_i^0;\vec{q}_i)D_b(a_i)S_0(E+q_{i-1}^0;\vec{q}_{i-1})\cdots$$
$$\times S_0(E+q_1^0;\vec{q}_1)V_C(\vec{a}_1)$$
$$\times\left\{\sum_{k=1}^{i-1}a_k^b\delta(a_n^0)\cdots\underline{\delta(a_i^0)}\cdots[\delta_+(a_k^0)\right.$$
$$-\delta_-(a_k^0)]\cdots\delta(a_1^0)$$
$$+\sum_{k=i+1}^{n}a_k^b\delta(a_n^0)\cdots[\delta_+(a_k^0)$$
$$\left.-\delta_-(a_k^0)]\cdots\underline{\delta(a_i^0)}\cdots\delta(a_1^0)\right\}. \tag{A93}$$

The $n-2$ delta functions in the first k-sum set $q_{n-1}^0=\cdots=q_i^0=0$, $q_{i-1}^0=\cdots=q_k^0$, and $q_{k-1}^0=\cdots=q_1^0=0$; while in the second k sum they require $q_{n-1}^0=\cdots=q_k^0=0$, $q_{k-1}^0=\cdots=q_i^0$, and $q_{i-1}^0=\cdots=q_1^0=0$. In either case we will use ω to represent the common value of the nonvanishing q^0s. We express the three-dimensional integrals in the usual implicit way, and obtain

$$\Delta G_T^{T(n)2}(E)=\frac{1}{2M}\sum_{i=1}^{n}\int d\omega[\delta_+(\omega)-\delta_-(\omega)]$$
$$\times\left\{\sum_{k=1}^{i-1}(V_CS_0(E))^{n-i}\vec{D}(\omega)S_0(E+\omega)(V_CS_0(E\right.$$
$$\left.+\omega))^{i-k-1}\cdot[\vec{p},V_C](S_0(E)V_C)^{k-1}\right.$$

$$- \sum_{k=i+1}^{n} (V_C S_0(E))^{n-k}[\vec{p},V_C]S_0(E+\omega)(V_C S_0(E + \omega))^{k-i-1} \cdot \vec{D}(\omega)(S_0(E)V_C)^{i-1} \Bigg\}. \quad \text{(A94)}$$

We now perform the sum over n, finding

$$\Delta G_T^{T2} = \frac{1}{2M} \int d\omega[\delta_+(\omega) - \delta_-(\omega)][1 - V_C S_0(E)]^{-1} \times \{\vec{D}(\omega)G_C(E+\omega) \cdot [\vec{p},V_C] - [\vec{p},V_C]G_C(E + \omega) \cdot \vec{D}(\omega)\} \times [1 - S_0(E)V_C]^{-1}. \quad \text{(A95)}$$

As before, an energy shift is obtained from a correction to G_T through Eq. (A23). We write the difference of the $\delta_\pm$ functions above as $2\delta_+(\omega) - \delta(\omega)$, and combine the two parts of ΔG_T^T to obtain the total one-transverse-photon energy correction

$$\Delta \mathcal{E}^T = \frac{-1}{2M}\left\langle \vec{D}(0) \cdot \vec{p} + \vec{p} \cdot \vec{D}(0)\right\rangle + \frac{1}{M} \int d\omega \delta_+(\omega)\langle \vec{D}(\omega)G_C(\mathcal{E}_0 + \omega) \cdot [\vec{p},V_C] - [\vec{p},V_C]G_C(\mathcal{E}_0 + \omega) \cdot \vec{D}(\omega)\rangle. \quad \text{(A96)}$$

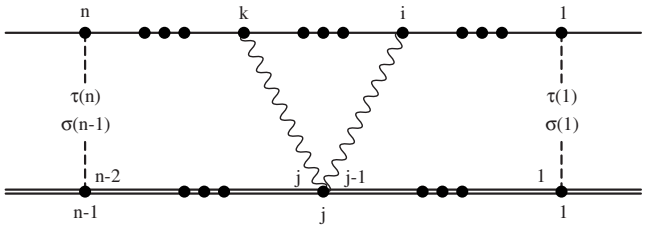

FIG. 10. A typical transverse-seagull graph with $n-2$ Coulomb photons. The numbers above the upper (electron) line label the photons connected to that line. The numbers below the lower (nucleus) line order the vertices on that line. As before, photon k (labeled by its position on the electron line) connects to position $\tau(k)$ on the nucleus line, and photon $\sigma(m)$ connects to position m on the nucleus line. The numbers just above the nucleus line label the $n-2$ individual nucleus propagators.

5. Transverse-seagull contribution

The graphs containing two transverse photons in a seagull configuration, along with an arbitrary number of Coulomb photons, comprise the final part of the $1/M$ recoil correction. A typical such graph is shown in Fig. 10. The contribution of all nth-order seagull graphs is

$$\Delta G_T^{S(n)}(E;\vec{p}_f,\vec{p}_i) = 2i\gamma^0 \int \frac{d^4q_1}{(2\pi)^4} \cdots \frac{d^4q_{n-1}}{(2\pi)^4} \sum_{i,k=1(k>i)}^{n} (-ie\gamma^0)[iS_0(E+q_{n-1}^0;\vec{q}_{n-1})\gamma^0](-ie\gamma^0) \cdots [iS_0(E+q_k^0;\vec{q}_k)\gamma^0](-ie\gamma^a)[iS_0(E + q_{k-1}^0;\vec{q}_{k-1})\gamma^0](-ie\gamma^0) \cdots [iS_0(E+q_i^0;\vec{q}_i)\gamma^0](-ie\gamma^b)[iS_0(E+q_{i-1}^0;\vec{q}_{i-1})\gamma^0](-ie\gamma^0) \cdots [iS_0(E+q_1^0;\vec{q}_1)\gamma^0] \times (-ie\gamma^0)\frac{i}{\vec{a}_n^2} \cdots \underline{k} \cdots \underline{i} \cdots \frac{i}{\vec{a}_1^2} iD_{aa'}(a_k)iD_{bb'}(a_i)(2\pi)^{n-2} \sum_{\text{partitions } X,Y} \{X\}_-\{Y\}_+(iZe)^{n-2}\left(i(iZe)^2\frac{\delta_{a'b'}}{2M}\right), \quad \text{(A97)}$$

where the initial two accounts for the two possible orderings of i and k on the electron line, and X and Y are partitions of $\{a_n^0, \ldots, \underline{a_k^0}, \ldots, \underline{a_i^0}, \ldots, a_1^0\}$. The partition sum gives a factor of $\delta(a_n^0)\cdots\underline{\delta(a_k^0)}\cdots\underline{\delta(a_i^0)}\cdots\delta(a_1^0)$, which sets $q_{n-1}^0 = \cdots = q_k^0 = 0$, $q_{k-1}^0 = \cdots = q_i^0 \equiv \omega$, and $q_{i-1}^0 = \cdots = q_1^0 = 0$. We make use of these delta functions to perform the energy integrals, and obtain

$$\Delta G_T^{S(n)}(E;\vec{p}_f,\vec{p}_i) = \frac{i}{2\pi M} \sum_{i,k=1(k>i)}^{n} \int \frac{d^3q_1}{(2\pi)^3} \cdots \frac{d^3q_{n-1}}{(2\pi)^3} \int d\omega V_C(\vec{a}_n)S_0(E;\vec{q}_{n-1}) \cdots S_0(E,\vec{q}_k)\vec{D}(a_k)S_0(E+\omega;\vec{q}_{k-1}) \cdots S_0(E + \omega;\vec{q}_i)\vec{D}(a_i)S_0(E;\vec{q}_{i-1}) \cdots S_0(E;\vec{q}_1)\vec{V}_C(\vec{a}_1). \quad \text{(A98)}$$

With implicit three-momentum integrals this becomes

$$\Delta G_T^{S(n)}(E) = \frac{i}{2\pi M} \sum_{i,k=1(k>i)}^{n} \int d\omega (V_C S_0(E))^{n-k}\vec{D}(\omega) \times S_0(E+\omega)(V_C S_0(E+\omega))^{k-i-1} \cdot \vec{D}(\omega) \times (S_0(E)V_C)^{i-1}. \quad \text{(A99)}$$

After summing over n this contribution takes the form

$$\Delta G_T^S(E) = \frac{i}{2\pi M} \int d\omega[1 - V_C S_0(E)]^{-1}\vec{D}(\omega)G_C(E+\omega) \cdot \vec{D}(\omega) \times [1 - S_0(E)V_C]^{-1}, \quad \text{(A100)}$$

and the corresponding energy shift is

$$\Delta \mathcal{E}^S = \frac{i}{2\pi M} \int d\omega \langle \vec{D}(\omega)G_C(\mathcal{E}_0 + \omega) \cdot \vec{D}(\omega)\rangle. \quad \text{(A101)}$$

6. Complete all-orders formula

In this section we will combine our pure-Coulomb, one-transverse-photon, and transverse-seagull contributions to obtain the full recoil corrections in an elegant form first written down by Yelkhovsky [21].

The pure-Coulomb contribution, from Eq. (A83), is

$$\Delta\mathcal{E}^C = \left\langle \frac{\vec{p}^2}{2M} \right\rangle + \frac{2\pi i}{M}\int d\omega \delta_+^2(\omega)\langle [\vec{p},V_C]G_C(\mathcal{E}_0 + \omega)\cdot[\vec{p},V_C]\rangle. \tag{A102}$$

The first term here is the leading recoil correction, contributing at $O((Z\alpha)^2 m^2/M)$ and containing only even powers of $Z\alpha$. The integral is of $O((Z\alpha)^5 m^2/M)$ as explicitly evaluated in Sec. IV in the leading one-loop approximation. For the full integral, which we denote I^C, we have

$$I^C = \frac{2\pi i}{M}\int d\omega \frac{(i/2\pi)^2}{(\omega+i\epsilon)^2}\left\langle [\vec{p},V_C]\left\{ \sum_{m(\mathcal{E}_{0m}>0)} \frac{\psi_{0m}\psi_{0m}^\dagger}{\mathcal{E}_0+\omega-\mathcal{E}_{0m}+i\epsilon} + \sum_{m(\mathcal{E}_{0m}<0)} \frac{\psi_{0m}\psi_{0m}^\dagger}{\mathcal{E}_0+\omega-\mathcal{E}_{0m}-i\epsilon} \right\} \cdot [\vec{p},V_C] \right\rangle. \tag{A103}$$

The positive energy term vanishes since we can close the ω contour in the upper half-plane. The negative energy contribution is

$$I^C = \frac{1}{M}\left\langle [\vec{p},V_C] \sum_{m(\mathcal{E}_{0m}<0)} \frac{\psi_{0m}\psi_{0m}^\dagger}{(\mathcal{E}_0-\mathcal{E}_{0m})^2}\cdot[\vec{p},V_C] \right\rangle. \tag{A104}$$

Now the commutators can be reduced using $H=\vec{\alpha}\cdot\vec{p}+\beta m + V_C$ and $[\vec{p},V_C]=[\vec{p},(H-\mathcal{E}_0)]$, so that

$$I^C = \frac{-1}{M}\left\langle \vec{p}(H-\mathcal{E}_0)\sum_{m(\mathcal{E}_{0m}<0)} \frac{\psi_{0m}\psi_{0m}^\dagger}{(\mathcal{E}_0-\mathcal{E}_{0m})^2}(H-\mathcal{E}_0)\cdot\vec{p} \right\rangle = -\frac{1}{M}\langle \vec{p}\Lambda_-\cdot\vec{p}\rangle, \tag{A105}$$

where

$$\Lambda_+ = \sum_{m(\mathcal{E}_{0m}>0)} \psi_{0m}\psi_{0m}^\dagger,$$

$$\Lambda_- = \sum_{m(\mathcal{E}_{0m}<0)} \psi_{0m}\psi_{0m}^\dagger, \tag{A106}$$

are the positive and negative energy projection operators. So the pure-Coulomb contribution can be written as

$$\Delta\mathcal{E}^C = \left\langle \frac{\vec{p}^2}{2M} \right\rangle - \frac{1}{M}\langle \vec{p}\Lambda_-\cdot\vec{p}\rangle = \frac{1}{2M}\langle \vec{p}(\Lambda_+-\Lambda_-)\cdot\vec{p}\rangle. \tag{A107}$$

Another form for the pure-Coulomb contribution is

$$\Delta\mathcal{E}^C = \frac{i}{2\pi M}\int d\omega \langle \vec{p}G_C(\mathcal{E}_0+\omega)\cdot\vec{p}\rangle. \tag{A108}$$

When the ω integral is done (taking care to include the contributions of infinite semicircles in the upper or lower half-planes), one finds immediately that Eq. (A108) agrees with Eq. (A107).

The one-transverse-photon contribution is

$$\Delta\mathcal{E}^T = \frac{-1}{2M}\left\langle \vec{D}(0)\cdot\vec{p}+\vec{p}\cdot\vec{D}(0)\right\rangle + \frac{1}{M}\int d\omega \delta_+(\omega)\langle \vec{D}(\omega)G_C(\mathcal{E}_0+\omega)\cdot[\vec{p},V_C]-[\vec{p},V_C]G_C(\mathcal{E}_0+\omega)\cdot\vec{D}(\omega)\rangle. \tag{A109}$$

The first commutator here can be written as $[\vec{p},V_C]\to -(H-\mathcal{E}_0)\vec{p}=-[H-(\mathcal{E}_0+\omega)]\vec{p}-\omega\vec{p}=G_C^{-1}(\mathcal{E}_0+\omega)\vec{p}-\omega\vec{p}$, with a similar form for the second commutator, so the integral in $\Delta\mathcal{E}^T$ takes the form

$$I^T = \frac{-1}{M}\int \frac{d\omega}{2\pi i}\frac{1}{\omega+i\epsilon}\langle \vec{D}(\omega)\cdot\vec{p}-\omega\vec{D}(\omega)G_C(\mathcal{E}_0+\omega)\cdot\vec{p} + \vec{p}\cdot\vec{D}(\omega)-\omega\vec{p}G_C(\mathcal{E}_0+\omega)\cdot\vec{D}(\omega)\rangle. \tag{A110}$$

Now an application of the residue theorem yields

$$\int \frac{d\omega}{2\pi i}\frac{1}{\omega+i\epsilon}\vec{D}(\omega;\vec{k}) = -\frac{1}{2}\vec{D}(0;\vec{k}), \tag{A111}$$

so the first term in Eq. (A109) cancels against part of I^T to yield

$$\Delta\mathcal{E}^T = \frac{-i}{2\pi M}\int d\omega \langle \vec{D}(\omega)G_C(\mathcal{E}_0+\omega)\cdot\vec{p}+\vec{p}G_C(\mathcal{E}_0+\omega)\cdot\vec{D}(\omega)\rangle. \tag{A112}$$

The three contributions to $\Delta\mathcal{E}$, expressed in Eqs. (A108), (A112), and (A101), combine to give the elegant final result

$$\Delta\mathcal{E} = \frac{i}{2\pi M}\int d\omega \langle (\vec{p}-\vec{D}(\omega))G_C(\mathcal{E}_0+\omega)\cdot(\vec{p}-\vec{D}(\omega))\rangle. \tag{A113}$$

[1] G. S. Adkins and J. Sapirstein, Phys. Rev. A **73**, 032505 (2006).
[2] G. P. Lepage, Phys. Rev. A **16**, 863 (1977).
[3] P. Beiersdorfer, H. Chen, D. B. Thorn, and E. Träbert, Phys. Rev. Lett. **95**, 233003 (2005).
[4] M. H. Chen, K. T. Cheng, P. Beiersdorfer, and J. Sapirstein, Phys. Rev. A **68**, 022507 (2003).
[5] E. Träbert, P. Beiersdorfer, K. B. Fournier, and M. H. Chen, Can. J. Phys. **83**, 829 (2005).
[6] E. E. Salpeter, Phys. Rev. **87**, 328 (1952).

[7] M. A. Braun, Zh. Eksp. Teor. Fiz. **64**, 413 (1973). [Sov. Phys. JETP **37**, 211 (1973)].
[8] V. M. Shabaev, Teor. Mat. Fiz. **63**, 394 (1985). [Theor. Math. Phys. **63**, 588 (1985)].
[9] W. R. Johnson, S. A. Blundell, and J. Sapirstein, Phys. Rev. A **37**, 307 (1988).
[10] J. Sapirstein and W. R. Johnson, J. Phys. B **29**, 5213 (1996).
[11] A. N. Artemyev, V. M Shabaev, and V. A. Yerokhin, Phys. Rev. A **52**, 1884 (1995).
[12] A. N. Artemyev, V. M. Shabaev, and V. A. Yerokhin, J. Phys. B **28**, 5201 (1995).
[13] G. P. Lepage, J. Comput. Phys. **27**, 192 (1978).
[14] M. Doncheski, H. Grotch, and G. W. Erickson, Phys. Rev. A **43**, 2152 (1991).
[15] G. S. Adkins and J. Sapirstein, Phys. Rev. A **58**, 3552 (1998).
[16] G. W. F. Drake and R. A. Swainson, Phys. Rev. A **41**, 1243 (1990).
[17] V. A. Yerokhin, P. Indelicato, and V. M. Shabaev, Phys. Rev. Lett. **91**, 073001 (2003).
[18] K. Melnikov and A. Yelkhosky, Phys. Lett. B **458**, 143 (1999).
[19] K. Pachucki and S. G. Karshenboim, Phys. Rev. A **60**, 2792 (1999).
[20] K. Pachucki and H. Grotch, Phys. Rev. A **51**, 1854 (1995).
[21] A. S. Yelkhovsky, JETP **83**, 230 (1996).
[22] W. E. Caswell and G. P. Lepage, Phys. Lett. **167B**, 437 (1986).
[23] T. Kinoshita and M. Nio, Phys. Rev. D **53**, 4909 (1996).
[24] S. J. Brodsky, in *Atomic Physics and Astrophysics*, edited by M. Chrétien and E. Lipworth (Gordon and Breach, New York, 1971), p. 92.